Chemical Science

ROYAL SOCIETY OF CHEMISTRY

PERSPECTIVE

View Article Online
View Journal | View Issue



Cite this: *Chem. Sci.*, 2022, **13**, 13657

All publication charges for this article have been paid for by the Royal Society of Chemistry

# Multipronged diagnostic and therapeutic strategies for Alzheimer's disease

Madhu Ramesh and Thimmaiah Govindaraju *

Alzheimer's disease (AD) is a progressive neurodegenerative disorder and a major contributor to dementia cases worldwide. AD is clinically characterized by learning, memory, and cognitive deficits. The accumulation of extracellular amyloid β (Aβ) plaques and neurofibrillary tangles (NFTs) of tau are the pathological hallmarks of AD and are explored as targets for clinical diagnosis and therapy. AD pathology is poorly understood and there are no fully approved diagnosis and treatments. Notwithstanding the gap, decades of research in understanding disease mechanisms have revealed the multifactorial nature of AD. As a result, multipronged and holistic approaches are pertinent to targeting multiple biomarkers and targets for developing effective diagnosis and therapeutics. In this perspective, recent developments in Aβ and tau targeted diagnostic and therapeutic tools are discussed. Novel indirect, combination, and circulating biomarkers as potential diagnostic targets are highlighted. We underline the importance of multiplexing and multimodal detection of multiple biomarkers to generate biomarker fingerprints as a reliable diagnostic strategy. The classical therapeutics targeting Aβ and tau aggregation pathways are described with bottlenecks in the strategy. Drug discovery efforts targeting multifaceted toxicity involving protein aggregation, metal toxicity, oxidative stress, mitochondrial damage, and neuroinflammation are highlighted. Recent efforts focused on multipronged strategies to rationally design multifunctional modulators targeting multiple pathological factors are presented as future drug development strategies to discover potential therapeutics for AD.

Received 14th July 2022
Accepted 13th October 2022

DOI: 10.1039/d2sc03932j

rsc.li/chemical-science

*Bioorganic Chemistry Laboratory, New Chemistry Unit, Jawaharlal Nehru Centre for Advanced Scientific Research, Jakkur P.O., Bengaluru, Karnataka 560064, India. E-mail: tgraju@jncasr.ac.in*

*Madhu Ramesh received his BVSc & AH in 2015 from Veterinary College, Bidar, Karnataka and MVSc in Biochemistry from Indian Veterinary Research Institute (IVRI), Bareilly, Uttar Pradesh, India. He joined JNCASR in 2017 for the PhD programme under the supervision of Prof. T Govindaraju. His research interests include understanding the pathophysiology and developing diagnostic and multifunctional therapeutic agents for Alzheimer's disease.*

*Thimmaiah Govindaraju is a Professor at the Bioorganic Chemistry Laboratory, New Chemistry Unit, JNCASR, Bengaluru, India. He received his MSc (2000) from Bangalore University and PhD in Chemistry (2006) from the National Chemical Laboratory and University of Pune, India. He carried out postdoctoral research at the University of Wisconsin-Madison, USA (2005–2006) and the Max Planck Institute of Molecular Physiology, Dortmund, Germany (2006–2008) as an Alexander von Humboldt postdoctoral fellow. His research interests are at the interface of chemistry, biology and biomaterials science, including Alzheimer's disease, peptide chemistry, molecular probes, theranostics, molecular architectonics, nanoarchitectonics, and silk and cyclic dipeptide derived biomimetics.*

## 1. Introduction

Dementia is a major cause of death globally and 70–80% of all cases are linked to AD.[1] There are more than 55 million people suffering from dementia worldwide, which are expected to grow to 139 million by 2050.[2] Over the decades, the number of deaths by leading diseases show a decreasing trend owing to the availability of reliable diagnostic and therapeutic interventions, while the deaths from AD increased by more than 145%.[1,2] Clinically AD patients show learning and memory impairment, language problems, and cognitive deficits leading to fatality within 5 to 12 years of disease diagnosis based on behavioural and cognitive symptoms.[3] Pathologically, AD is characterized by the extracellular Aβ senile plaques and NFTs of hyper-phosphorylated tau protein, associated neurodegeneration, and brain atrophy.[4] AD etiopathology has been described by the cholinergic hypothesis, amyloid hypothesis, and tau hypothesis over the last three decades. Recent discoveries have uncovered the complex pathobiology and showed the multifactorial nature of AD (Fig. 1).[4–9] The accumulating evidence demonstrates the role of metal ion dyshomeostasis, reactive oxygen species (ROS), oxidative stress, mitochondrial damage, and neuro-inflammation in the pathology of AD.[10]

Aβ and tau aggregation species are the hallmarks of AD and targeted for diagnosis over the last two decades using different chemical tools with positron emission tomography (PET), magnetic resonance imaging (MRI), and fluorescence imaging techniques. The advancements in PET probes and the technique allow the clinical detection of Aβ and tau biomarkers.[11] Aβ and tau PET imaging suffer from a few limitations like the requirement of clinical experts, cost, sophisticated instrumentation, radiation hazard, differential diagnosis, and failure to provide definite disease diagnosis at the early stage. Recently, the National Institute on Aging and Alzheimer's Association (NIA-AA) has set a framework, wherein the use of definitive core biomarkers like Aβ (A), tau (T), and neurodegeneration (N) is advocated for AD diagnosis.[12] The proposed biomarker list is left open-ended to allow the addition of newly validated biomarkers. The multiple pathological pathways of AD emphasise the potential of considering novel and multiple biomarkers associated with disease pathology for early and accurate diagnosis. The disease-associated markers circulating in the fluids like cerebrospinal fluid (CSF), blood, saliva, and urine hold potential for disease diagnosis. Thus, circulating biomarkers have been explored in recent years owing to numerous advantages over imaging techniques.[13] Recently, many multicentric clinical studies have identified promising circulating biomarkers in CSF and blood for their utility in routine screening in large clinical cases. We proposed multiplexed detection of multiple biomarkers using multimodal imaging and detection techniques to generate a signature fingerprint of biomarkers. The signature fingerprint aids early diagnosis and categorises different clinical stages with high accuracy for personalised medication and effective therapeutic intervention.[14]

AD drug developments have been revolving around cholinergic and amyloid hypothesis over the last three decades.[15] Currently, drugs available to treat AD provide only symptomatic relief and do not directly target the underlying disease mechanisms. The therapeutic targeting of Aβ met with failures due to intervention at advanced stages and the multifactorial nature of AD. Aducanumab, a monoclonal antibody (mAb), has been conditionally approved for therapeutic targeting of Aβ in AD patients with mixed output.[16] Similarly, targeting tau

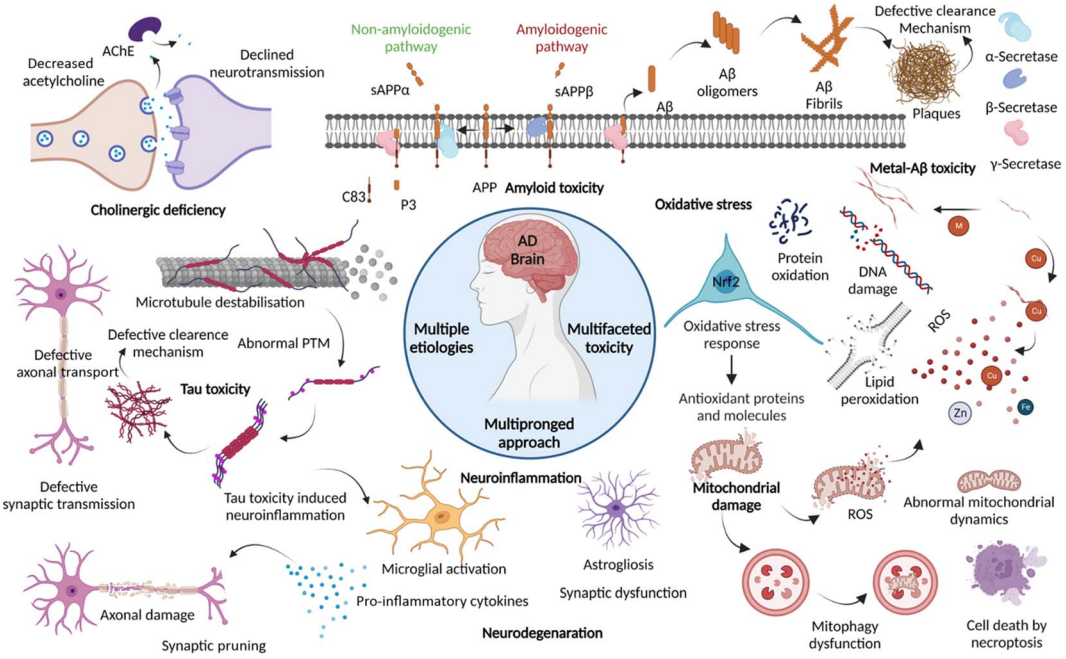


Fig. 1 Schematic representation of multiple aetiologies and multifaceted toxicity of AD, which emphasize the need to adopt multipronged approaches for the management of diagnosis and treatment (created with BioRender.com).

Table 1 Diagnostic tools and techniques targeting core and indirect biomarkers for AD[a]

| Sl. no. | Diagnostic markers and techniques | Chemical probe/ techniques | Characteristic features | | | | | Model tested | Ref. |
|---|---|---|---|---|---|---|---|---|---|
| 1 | **Aβ targeted diagnostics** | | | | | | | | |
| | **NIRF imaging** | | $\lambda_{ex}$ | $\lambda_{em}$ | $\phi$ | **Fold** | $K_d$ | | |
| | Oligomers | BD-Oligo | 530 | — | — | 6 | 0.48 μM | Tg M | 20 |
| | | F-SLOH | — | 650 | — | — | 1.13 μM | Tg M | 21 |
| | | PTO-29 | 570 | 680 | | 60 | 0.25 μM | Tg M | 22 |
| | Soluble aggregates/ protofibrils | DCM-AN | 500 | 661 | 0.015 | — | 0.85 μM | Tg M | 26 |
| | | CRANAD102 | 580 | 700 | 0.018 | 68 | 7.5 nM | Tg M | 28 |
| | Fibrils | TC | 537 | 638 | 0.4 | 30 | 58.4 nM | *In vitro* | 23 |
| | | CQ[b] | 516 | 664 | 0.36 | 100 | 84 nM | Human | 24 |
| | | PHC4 | — | 741 | 0.78 | 62.2 | 14.1 nM | Tg M/human | 27 |
| | | QM-FN-$SO_3$ | 500 | 720 | — | — | 170 nM | Tg M | 30 |
| | | ADlumin1 | — | 540 | — | 100 | 2.1 μM | Tg M | 31 |
| | | **18** | — | 618 | 0.31 | 223 | 43.1 nM | Tg M | 32 |
| | Different alloforms | QAD1 | Binds to monomers, oligomers, and fibrils | | | | | Tg M | 25 |
| | | Combinatorial molecular sensor | Differentiate different alloforms like monomer, oligomer, LMW, and HMW aggregates | | | | | *In vitro* | 29 |
| | **PET imaging** | | | | | | | | |
| | Fibrils | $^{11}$C-PiB | ThT based PET probe, approved for clinical use and a gold standard test | | | | | Human | 33 |
| | | $^{18}$F-flutemetamol | Fluorine-labelled analogue of PiB, approved for clinical use | | | | | Human | 34 |
| | | $^{18}$F-florbetaben | Stilbene–polyethylene glycol conjugate, selective labelling, approved for clinical use | | | | | Human | 35 |
| | | $^{18}$F-florbetapir | Highly selective, low background, good pharmacokinetics and correlates with post-mortem Aβ deposition | | | | | Human | 36 |
| | | $^{18}$F-FIBT | Imidabenzothiazole-based, high contrast and better than the reported probes | | | | | Tg M | 37 |
| | | $^{64}$Cu-HYR17 | Benzothiazole-based, Cu chelating probe with a better half-life | | | | | Tg M | 38 |
| | **MRI** | | | | | | | | |
| | Fibrils | USPIO-Aβ1–42 | Aβ conjugated to iron oxide NPs, micron-scale resolution, and map Aβ deposition | | | | | Tg M | 39 |
| | | HMON-abAβ40 | Aβ antibody conjugated with manganese NPs, image and monitor Aβ load | | | | | Tg M | 40 |
| 2 | **Tau targeted diagnostics** | | | | | | | | |
| | **NIRF imaging** | | $\lambda_{ex}$ | $\lambda_{em}$ | $\phi$ | **Fold** | $K_d$ | | |
| | Fibrils | PBB3 | 405 | 520 | — | — | 2.55 nM | Tg M/human | 42 |
| | | **2e** | 550 | 660 | — | 310 | 0.77 μM | Tg M | 43 |
| | | BD-tau | 525 | 590 | 0.3 | 3.2 | 0.89 μM | Tg M | 44 |
| | | Tau 1 | 633 | 742 | 0.92[b] | 6.4 | 2.77 μM | Tg M | 45 |
| | | Tau 2 | 607 | 723 | 0.84[b] | 9.3 | 6.18 μM | Tg M | |
| | | **2c** | 502 | 632 | 0.82 | 44 | 6.06 nM | Tg M | 46 |
| | | Q-tau 4 | 424 | 630 | 0.01 | 3.82 | 16.6 nM | Human | 47 |
| | | **18** | — | 711 | 0.019 | 50.2 | 33.2 nM | Tg M | 32 |
| | Soluble aggregates | pTP-TFE | 450 | 520 | 0.27 | — | 66 nM | Tg M | 48 |
| | **PET imaging** | | | | | | | | |
| | Fibrils | $^{18}$F-THK5117 | Arylquinoline based probe, good pharmacokinetics | | | | | Human | 49 |
| | | $^{18}$F-flortaucipir (Tauvid) | Indole based probe, selective labelling and approved for clinical use | | | | | Human | 50 |
| | | $^{18}$F-JNJ64349311 | Performs better than $^{18}$F-flortaucipir | | | | | Tg M | 51 |
| | | $^{18}$F-GTP1 | Highly selective with no MAO binding | | | | | Human | 52 |
| | | $^{18}$F-PI-2620 | High contrast, signal to noise ratio, accurately distinguish AD from healthy | | | | | Human | 53 |
| | **MRI** | | | | | | | | |
| | Tau tangles and tau positive cells | Shiga-X35 | $^{18}$F-MRI agent targeting tau tangles | | | | | Tg M | 54 |
| | | Tau-X | Aptamer based nanoformulation targeting hyperphosphorylated tau positive neurons | | | | | Tg M | 56 |

Table 1 (*Contd.*)

| Sl. no. | Diagnostic markers and techniques | Chemical probe/ techniques | Characteristic features | Model tested | Ref. |
|---|---|---|---|---|---|
| **3** | **Neurodegeneration** | | | | |
| | PET imaging | $^{18}$FDG–PET | Imaging metabolic activity of the brain | Human | 59 |
| | MRI | sMRI | Assessment of brain atrophy | Human | 61 |
| | | fMRI | Mapping functional connectivity of the brain | Human | 64 |
| **4** | **Indirect biomarker targeted diagnostics** | | | | |
| | TSPO PET imaging | $^{11}$C-PK11195 | First *in vivo* clinical TSPO PET imaging | Human | 67 |
| | | $^{11}$C-PBR28 | Correlates with Aβ and tau accumulation | Human | 68 |
| | SV2A PET imaging | $^{11}$C-UCB-J | First *in vivo* PET probe with biocompatibility | Human | 69 |
| | | $^{18}$F-UCB-H | Correlates with cognitive decline and Aβ load | Human | 70 |
| | | $^{18}$F-SynVesT-1 | Better pharmacokinetics and binding | Human | 71 |
| | | $^{18}$F-SynVesT-2 | High brain uptake, fast kinetics, and better binding | Human | 72 |
| | HOCl fluorescence imaging | CM2 | Fluorescent probe detects selectively HOCl, demonstrates elevated levels and proximal localisation of HOCl with Aβ in the AD brain | Tg M | 73 |
| | Metal ion MRI | Intrinsic Fe | Elevated Fe levels in the AD brain serve as a MRI contrast agent and its quantification | Human | 76 |

[a] Tg M – transgenic mouse model. [b] Antibody like selectivity and sensitivity to Aβ plaques with potential for differential diagnosis of AD from other tauopathies and neurodegenerative diseases as in the case of mixed dementia.

aggregation, modifications and clearance have drawn the attention of therapeutics development. Many of the tau-targeted therapeutic candidates are in clinical trials and their success is yet to be revealed.[8] Recent discoveries on AD etiopathology uncovered many tangible drug targets, which are anticipated to drive drug development in a faster mode. The lesson learned from the failures of Aβ and tau-targeted drug developments are a guide to developing multifunctional molecules to tackle multiple AD pathologies.[4,8,17–19] We propose rational development of multifunctional modulators targeting multiple disease mechanisms as a future therapeutics strategy to tackle multifactorial AD. In this perspective, we present multipronged diagnostic and therapeutic approaches, multiplexed and multimodal diagnosis, and rational design of multifunctional modulators of AD with a future outlook.

## 2. Diagnostic strategies

### 2.1 Clinical diagnosis of AD

Over the past two decades, there have been notable developments in identifying and validating reliable diagnostic methods and biomarkers for AD. The international working group (IWG) established a clinical-biological definition of AD, wherein the clinical phenotypes of cognitive impairment and biological biomarkers detected through *in vivo* imaging augment the diagnosis of AD. The clinical assessment of progressive decline in memory, impaired episodic memory, and cognitive changes along with support from biomarker positivity (ATN) has been employed for AD diagnosis.[3] The clinical symptoms are assessed using memory and cognitive tests like Montreal Cognitive Assessment (MoCA), Mini-Mental State Exam (MMSE) and Mini Cog by clinical experts. Various chemical probes and techniques like near infrared-fluorescence (NIRF), PET, and MR imaging are being utilised for ATN biomarker imaging (Tables 1 and 2).

### 2.2 Aβ (A) targeted diagnosis

**NIR fluorescent (NIRF) probes for Aβ imaging.** The accumulation of Aβ aggregates is prominently evident in the AD brain and various NIRF probes are developed for the detection and imaging of different alloforms of Aβ aggregates (Fig. 2A). Most of the probes target Aβ fibrils and few are designed as Aβ oligomer-targeting probes, as these oligomers play a critical role in AD pathology. The design of small molecule probes targeting oligomers is challenging due to poor structural information, and heterogenous and transient species. A Bodipy-based small molecule probe BD-Oligo was identified by the diversity-oriented fluorescence library approach and high content imaging screening to selectively target Aβ oligomers.[20] The probe was selective to oligomers ($K_d$ = 0.48 μM) and stain Aβ oligomer species in the APP/PSEN1 mouse model. Fluoro-substituted cyanine dye F-SLOH selectively binds and detects Aβ oligomers as revealed by *ex vivo* immunofluorescence in the Tg AD brain tissue with various antibodies (Aβ-Oligo, 6E10, 4G8, pAβ, and MC6) and the Aβ oligomer level was quantified by NIRF imaging.[21] Based on the 3D structure of Aβ oligomers, V-shaped NIRF probes PTO-9, 18, 26, and 29 were designed to fit in a unique triangular cavity made of Phe19/Val36.[22] Among all, PTO-29 successfully labels oligomers in a 4 month old APP/PSEN1 Tg mouse model. Aβ fibril targeting fluorescent probes have been developed as a diagnostic agent for AD (Fig. 2A). Donor–acceptor modality in molecular design has been extensively used for the development of fluorescent probes for the detection of Aβ aggregates. In this direction, we have developed a hemicyanine-based benzothiazole-coumarin (TC) probe as an

 

Table 2 Circulating biomarkers for the diagnosis of AD[a]

| Sl. no. | Biomarker class | Target biomarkers | Remarks | Specificity (%) | Sensitivity (%) | Sample size | Ref. |
|---|---|---|---|---|---|---|---|
| **1** | **CSF and blood** | | | | | | |
| | Aβ | Aβ42/40 | Decreased significantly, correlates with Aβ positivity | 100 | 84 | 45 | 91 |
| | | Composite model | Model from Aβ42, 40 and ratio diagnose disease with 90% accuracy | 81 | 96.7 | $N$ =121 and $N$ = 252 | 92 |
| | Tau | t-tau and p-tau | Increased | 80 | 80 | 97 | 94 |
| | | p-tau-181 | Increased, discriminate MCI and AD. Correlates with tau PET positivity, atrophy, and CSF biomarkers | 87 | 92 | $N1$ = 182 $N2$ = 344 | 95 |
| | | p-tau-217 | Increased 6-fold in AD correlates with Aβ and tau positivity, early diagnosis of AD | 91 | 91 | 194 + 32 | 96 |
| | | p-tau-231 | Increased in the early stage, outperforms p-tau-181, correlates with Aβ and tau deposition | — | — | 38 + 313 | 99 |
| | Protein biomarkers | Neurogranin | Increased in CSF and correlates with CSF biomarkers, atrophy and brain Aβ load | 60 | 79 | 302 | 100 |
| | | Synaptotagmin | Increased, discriminate MCI and AD | — | — | 39 + 78 | 102 |
| | | sTREM | Increased, correlates with CSF Aβ and tau biomarkers, atrophy and brain Aβ load | — | — | 155 + 93 | 103 |
| | | YKL-40 | Increased, correlates with Aβ deposition and memory deficits | 85 | 85 | 318 | 104 |
| | | Nf-L | Increased, correlates with CSF t-tau and p-tau, cortical atrophy, Aβ deposition and brain metabolism. Discriminate MCI and AD cases | | | CSF-187 Ser-405 $N$ = 196 | 106 |
| | RNA biomarkers | BACE1 lcnRNA | Increased in plasma | 61.3 | 87.5 | 134 | 109 |
| | | miRNA panels | Exosome 7 miRNA panel diagnoses with 89% accuracy (miR-185-5p, miR-342-3p, miR-141-3p, miR342-5p, miR-23b-3p, miR-338-3p and miR-3613-3p) | — | — | 70 | 110 |
| | | | Plasma 6 miRNA panel (miR-185-5p, miR-342-3p, miR-141-3p, miR342-5p, miR-23b-3p, miR-338-3p and miR-3613-3p) | 78 | 75 | 50 | 111 |
| | | | CSF 6–7 miRNA panel, correlates with CSF biomarkers and the cognitive score | — | — | 118 | 112 |
| | Protein and metabolite panel | Multiple protein panel in blood | 18 biomolecule alteration was identified (2 cohorts) | 93 85 | 85 80 | $N1$ = 961 $N2$ = 170 | 113 |
| | | 3 protein panel | Plasma Aβ42/40, pTau-217 and Nf-L diagnose AD and correlates with cognitive changes | — | — | 435 | 114 |
| | | 4 protein panel | Blood exosomal GAP43, neurogranin, SNAP25 and synaptotagmin-1 are early diagnosis biomarkers | — | — | 320 | 116 |
| | | Spingomyelin metabolites | 26 metabolites, diagnose AD with an accuracy of 83.33% | 80 | 86.67 | $N1$ = 44 $N2$ = 767 $N3$ = 207 | 117 |
| **2** | **Saliva** | | | | | | |
| | Aβ | Aβ42 | Increased and specific to AD over PD | — | — | 22 | 118 |
| | Tau | p-tau/t-tau | Increased | — | — | 59 | 119 |
| | | p-tau-396/t-tau | Increased, no correlation with other biomarkers | 50 | 73 | 148 | 120 |
| | Lf | Full length Lf | Decreased, outperforms CSF biomarkers. Other studies contradict and changes are inconsistent | 100 98.6 | 100 100 | $N1$ = 274 $N2$ = 127 | 121 |
| **3** | **Urine** | | | | | | |
| | Protein | SPP1, GSN and IGFBP7 | Increased, MS techniques were used to screen and confirmed by ELISA | — | — | 40 | 125 |

Table 2 (*Contd.*)

| Sl. no. | Biomarker class | Target biomarkers | Remarks | Specificity (%) | Sensitivity (%) | Sample size | Ref. |
|---|---|---|---|---|---|---|---|
| **4** | **Tear** | | | | | | |
| | Protein | Lipocalin-1, dermcidin, lysozyme-C and lacritin | Proteins are significantly altered in AD over healthy individuals<br>Significant increase in the tear total protein and flow rate | 77 | 81 | 23 | 124 |

[a] p-tau: phosphorylated tau and t-tau: total tau.

Aβ selective and sensitive NIRF probe (Fig. 2A).[23] Upon binding to Aβ fibrillar aggregates, TC displays high fluorescence enhancement and shift in the absorbance, which provided dual responsive properties with colorimetric and fluorescence readouts. TC exhibits selectivity and high binding affinity ($K_d$ = 58.43 nM) with 30-fold fluorescence enhancement to Aβ fibrillar aggregates compared to other protein aggregates. TC displayed a red shift in the absorbance spectrum (117 nm) with a visible colour change from pale pink to purple. A detailed computational study and competitive binding assay revealed that the probe binds to the thioflavin T (ThT) binding pocket and a shift in the local hydrophilic to hydrophobic microenvironment results in a red shift of absorbance and fluorescence enhancement. *In silico* analysis of molecular interactions revealed that TC exhibits hydrophobic interaction with the Leu17 and Val39 residues of fibrils and engage in π–π stacking with the phenyl ring of Phe19 in the fibrils. Furthermore, we developed a coumarin–quinoline (CQ) based NIR turn-on fluorescent probe with antibody-like selectivity and sensitivity to Aβ aggregates (Fig. 2A and B).[24] *In vitro* studies showed selective fluorescence enhancement of the CQ probe in the presence of Aβ aggregates compared to other biomolecules and protein aggregates (bovine serum albumin, calf thymus DNA, tau, α-synuclein and islet amyloid polypeptide) (Fig. 2B). The sensitivity of CQ was revealed by its high affinity binding to Aβ aggregates with $K_d$ = 86 nM and 100-fold fluorescence enhancement. The nonselective dye ThT is a commonly used green fluorescent probe to stain and image Aβ and other amyloid aggregates *in vitro* and the tissue sections. The probe CQ exhibits 10-fold higher selectivity over ThT and binds in the proximity of the ThT binding pocket as evidenced by the displacement assay and computational study. A molecular docking study revealed possible CQ binding to multiple sites, and among them binding to the entry cleft site was strong and

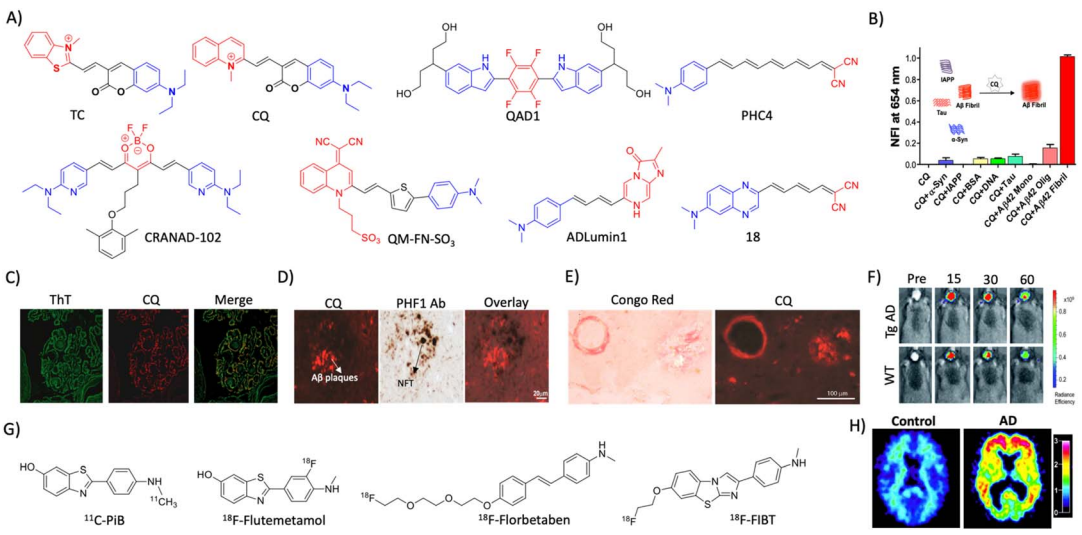


Fig. 2 Molecular probe targeting Aβ. (A) NIR fluorescent probes targeting Aβ fibrils (blue and red represent donor and acceptor moieties, respectively). (B) Selective fluorescence response of the CQ probe to Aβ aggregates in comparison with BSA and other amyloid protein aggregates. (C) Fluorescence staining of human brain tissue with CQ and ThT shows selective Aβ aggregate staining by CQ. (D) Immunofluorescence staining of human AD brain tissue shows the selective binding of CQ with Aβ aggregates over tau aggregates as reflected by poor colocalisation with PHF1 tau antibody staining. (E) CQ stain congophilic angiopathy similar to Congo red staining. (B)– (E) Reproduced from ref. 24 with permission from Elsevier, copyright 2017. (F) NIRF imaging of amyloid aggregates in the Tg AD mice model using CRANAD102 at different time interval (min) distinguish AD from WT. Reproduced from ref. 28 with permission from the Royal Society of Chemistry, copyright 2017. (G) Aβ fibril targeting PET probes. (H) PiB PET images of human healthy and AD brains. Reproduced from ref. 33 with permission from the American Neurological Association, copyright 2003.

stable. The binding of the probe was largely driven by van der Waals interactions for Aβ fibril:CQ complex formation. CQ is non-toxic to cells and crosses BBB which underscores its *in vivo* utility for non-invasive NIR imaging. The co-staining of human AD brain samples (*ex vivo*) with CQ and ThT demonstrated the selective labelling of Aβ plaques by CQ over other aggregates with a significantly minimal background signal compared to the latter (Fig. 2C). The probe showed poor localisation with NFT antibodies, which demonstrates its ability to differentiate AD from other tauopathies (Fig. 2D). The probe neatly stains the congophilic aggregates and vascular amyloids (Fig. 2E). CQ has the potential to be used for differential diagnosis of AD over tauopathies and other neurodegenerative disorders as in the case of mixed dementia.

A photoinduced electron transfer (PIET) quenched NIRF probe QAD1 was designed with Bodipy as the fluorophore and tetrahydroxyquinoxaline as the quenching moiety.[25] The probe exhibits turn-on fluorescence upon interaction with different Aβ alloforms, which was used to detect and monitor Aβ load in a 6-month-old APP/PSEN1 Tg mouse model. Recently, DCM-AN was designed by combining the dicyanomethylene (DCM) skeleton with an Aβ targeting aminonaphthalene (AN) moiety, which showed selectivity towards protofibrils.[26] Molecular dynamics (MD) simulation of the probe with trimer (oligomers), dodecamer (protofibrils) and fibrillar structures revealed strong binding towards the dodecamer, which suggests selectivity towards protofibrils. Upon binding to protofibrils, the rotation of both ethylene and piperidine groups of the probe is restrained, which results in fluorescence enhancement. The probe detects protofibrils in the *ex vivo* brain sections at different stages in the Tg AD mouse model. The donor–acceptor (D–A) architecture was expanded by playing around with the π-bridge, donor aromatic moieties, and dicyano moiety as the acceptor.[27] Among them, PHC4 exhibits favourable properties with *in vivo* NIRF imaging to distinguish between WT and Tg AD mice. Ran *et al.* tuned the steriohindrance of curcumin at the phenoxy alkyl chain to make the probes selective to soluble Aβ aggregates.[28] Among them, CRANAD102 exhibited selectivity (68-fold over insoluble aggregates) to soluble aggregates with a strong binding affinity ($K_d$ = 7.5 nM). The probe was successfully utilised for *in vivo* NIRF imaging of the soluble aggregates in the early stage (4 months) of the Tg AD mouse model, which allowed monitoring of the changes over 4 to 12 months (Fig. 2F).

Margulies *et al.* have reported a combinatorial sensor for the detection of various Aβ alloforms.[29] The sensor was constructed by conjugating three fluorescent probes ThT, sulforhodamine B, and sulfo Cy5 onto a proline scaffold with a KLVFF moiety. The sensor was employed to detect different alloforms *viz.*, monomers, low molecular weight (LMW) and higher molecular weight (HMW) oligomers, and aggregates, based on differential fluorescence response due to varied intramolecular FRET among fluorophores. Recently, an aggregation-induced emission (AIE) based probe QM-FN-$SO_3$ was developed by connecting DCM-N with dimethylaminobenzene through a π-conjugated thiophene bridge and introduced a sulphonate moiety as a substitution that keeps the probe in the off state.[30] The thiophene bridge with π-conjugation retains the lipophilicity to enhance the BBB permeability and NIR emission of the probe. QM-FN-$SO_3$ aggregates on the hydrophobic surface of Aβ aggregates and exhibits a turn-on fluorescence response. The AIE probe was BBB permeable and mapped Aβ aggregates with high fidelity in the Tg AD mouse model. A novel turn-on chemiluminescent probe ADlumin1 was designed to target Aβ aggregates.[31] The discrimination of AD from WT was improved by dually amplifying the signal *via* chemiluminescence resonance energy transfer (DUS-CRET) between CRANAD-3 and ADlumin1 in a 5-month-old 5xFAD mouse model. The simultaneous detection of both Aβ and tau aggregates would enhance the accuracy of AD diagnosis. D–A based probe **18** with environmental sensitivity can differentially emit fluorescence in the presence of brain-derived Aβ and tau aggregates.[32] Probe **18** successfully discriminates Aβ and tau aggregates in Tg mouse models and measure the load *in vivo* through NIRF imaging.

**Aβ PET imaging.** PET imaging of Aβ deposits has been pursued for the last two decades and currently, there are a few probes approved for clinical diagnosis (Fig. 2G). The first known Aβ PET tracer PiB with a $^{11}C$ isotope (half-life = 20.34 min) was developed by Klunck *et al.*, at the University of Pittsburgh.[33] In 2013, PiB received FDA approval for the clinical diagnosis of AD and to date, it has been considered as a gold standard for Aβ PET imaging that correlates with post-mortem Aβ deposits (Fig. 2H). Fluorine ($^{18}F$) labelled radiotracers flutemetamol ($^{18}F$-GE-067), florbetaben (BAY-94-9172), and florbetapir ($^{18}F$-AV-45) with a better half-life (109.8 min) and the least background noise have been developed for Aβ plaques (Fig. 2G). Flutemetamol was successful in labelling Aβ plaques in AD patients and diagnosed with high sensitivity and specificity in an advanced stage of disease and approved for clinical use.[34] Florbetaben, a stilbene-based probe conjugated with polyethylene glycol, shows selectivity for Aβ plaques over other aggregates, which received FDA approval owing to its safety and diagnostic potential.[35] The benzene ring in the stilbene moiety was replaced with a pyridine ring to derive florbetapir, which exhibits a low background signal and high diagnostic accuracy.[36] An imidazobenzothiazole based $^{18}F$-labelled PET probe $^{18}F$-FIBT performed better than reported probes.[37] Clinical studies reveal the safety and the diagnostic utility of $^{18}F$-FIBT as a next-generation Aβ PET probe. Recently, copper ($^{64}Cu$) based PET probes have been designed for Aβ aggregates due to its high half-life (12.8 h). Benzothiazole based Cu chelating ligands bind to Aβ aggregates and strongly chelate Cu that acts as a PET probe.[38] The probes were constructed by conjugating a metal (Cu) chelating group, triazacyclononane (tacn), with Aβ targeting, substituted benzothiazole moiety. Among them, HYR17 showed good brain uptake and labelled Aβ aggregates to distinguish Tg AD mice from WT.

**Aβ MR imaging.** MR imaging was carried out to analyse the brain connectivity and atrophy that are signatures of neurodegeneration. Structural and functional MRI was adopted to assess atrophy and brain activity, respectively. MR imaging agents targeting Aβ are minimal unlike NIRF and PET probes for the diagnosis of AD. Ultrasmall superparamagnetic iron oxide (USPIO) nanoparticles were conjugated with the Aβ42

peptide to make a USPIO-Aβ1–42 MRI probe that targets Aβ aggregates.[39] USPIO-Aβ1–42 with mannitol as a contrast agent was used to image at micron resolution in an APP/PSEN1 Tg mouse model. In another study, an MRI agent was prepared by conjugating an antibody for Aβ (HMON-abAβ40) with manganese nanoparticles. The novel MRI agent was successfully used for imaging and monitoring Aβ load in the Tg AD mouse model.[40] A gadolinium-based contrast agent has been used as a non-targeted contrast and utilised for MR imaging of the Tg AD mouse brain.[41] This probe was able to enhance the contrast for Aβ aggregates. The clinical utility of MRI agents targeting Aβ is yet to be evaluated and adapted for AD diagnosis.

### 2.3 Tau (T) targeted diagnosis

**NIRF probes for tau imaging.** Tau is an intrinsically disordered protein aggregate to form different alloforms. Several NIR fluorescent probes were developed targeting tau for the detection and diagnosis of AD (Fig. 3A). Inspired from ThT, a set of phenyl/pyridinyl-butadienyl-benzothiazoles/benzothiazolium probes (PBBs) were designed by introducing two π-chain bridge between aniline and benzothiazole moieties.[42] Among all, PBB3 with optimal properties was BBB permeable and successfully utilised to label the tau aggregates in the Tg mouse model. Radiolabelled $^{11}$C-PBB3 was successful in the Tg AD mouse model and clinical human subjects to discriminate between AD and healthy subjects. A series of fluorescent probes were synthesised by conjugating distinctly substituted difluoroboron β-ketonate with *N*,*N*-dimethylaniline.[43] Among them, **2e** showed 310-fold fluorescence enhancement with tau aggregates. The cellular imaging with SH-SY5Y cells expressing GFP-tau and immunofluorescence in human AD brain samples shows colocalisation with phosphorylated tau (p-tau) antibodies reflecting its selective tau staining. A Bodipy-based live cell imaging probe BD-tau was evolved through a diversity-oriented fluorescence library approach (DOFLA).[44] BD-tau showed fluorescence enhancement (3.2 fold) selectively to tau aggregates and successfully stains tau tangles in the brain sections of the Tg mouse model. BAP1, an Aβ probe was modified with extended conjugation to develop two probes tau 1 and tau 2 to target tau aggregates.[45] Tau 1 is biocompatible, crosses BBB, and selectively stains p-tau aggregates in a tau mouse model (Fig. 3B). Molecular docking studies with the VQIVYK crystal structure revealed that the probe tightly fits in the tunnel architecture along the fibril axis. *In vivo* NIRF imaging showed that the probe could distinguish the Tg tau mouse model from age-matched WT animals (Fig. 3C). A series of Bodipy-based probes were designed using *N*,*N*-dimethylaminobenzene as a donor and the $BF_2$ benzamide group as the acceptor bridged with the π-chain.[46] Probe **2c** showed good fluorescence enhancement with nanomolar binding affinity with Aβ and tau aggregates. *In vivo* NIRF imaging with **2c** discriminates 22-month-old WT and AD Tg mouse models. Inspired by THK family PET tracers, push–pull fluorescent probes composed of dimethylaminophenyl/pyridinyl as the donor and the quinoline moiety as the acceptor group with a π-bridge were designed.[47] Among them, Q-tau 4 exhibits strong intramolecular charge

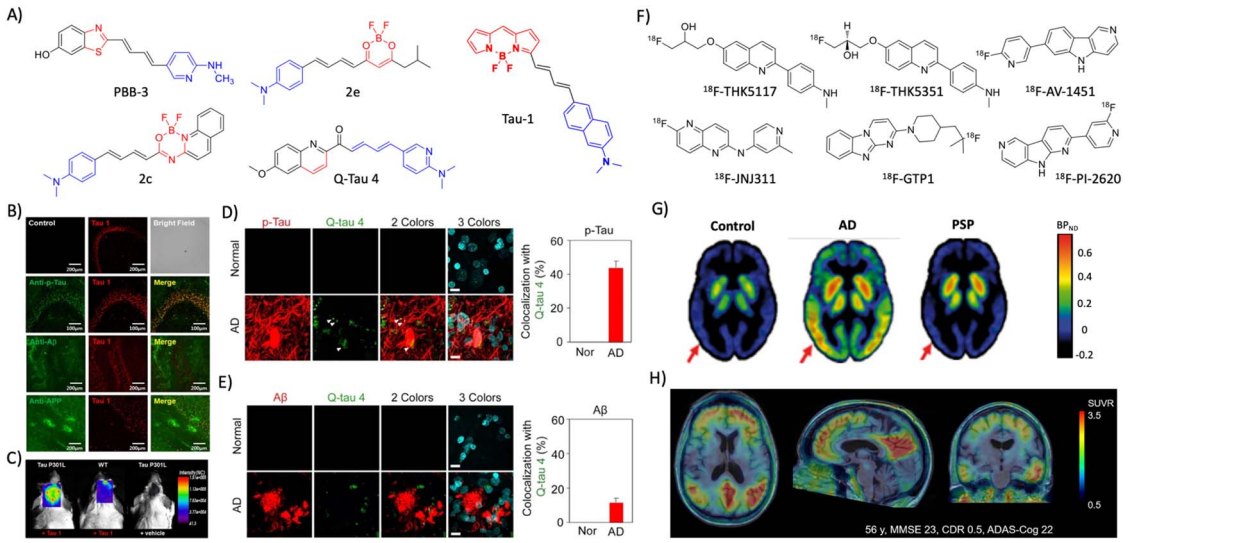


Fig. 3 Molecular probes targeting tau. (A) NIR fluorescent probes targeting tau fibrils (blue and red represent donor and acceptor moieties, respectively). (B) Immunofluorescence imaging in a 3xTg mice brain with antibodies targeting tau aggregates, Aβ, and APP protein shows the selective tau labelling by tau 1 (scale bar 200 μm). (C) NIRF imaging of tau aggregates by tau 1 in a Tg mouse after 30 min of injection. (B) and (C) Reproduced from ref. 45 with permission from the American Chemical Society, copyright 2017. (D) *Ex vivo* immunofluorescence imaging of normal heathy and AD human brain tissues with Q-tau 4 and its colocalisation with the p-tau antibody (scale bar 20 μm). (E) *Ex vivo* fluorescence imaging of normal healthy and AD human brain tissues with Q-tau 4 and Aβ antibodies. Quantification shows the poor colocalisation indicating the selective tau labelling by the probe (scale bar 20 μm). (D) and (E) Reproduced from ref. 47 with permission from the American Chemical Society, copyright 2021. (F) Tau targeting PET probes. (G) PET images of control, AD, and PSP human subjects obtained by using the $^{18}$F-AV-1451 probe. Reproduced from ref. 50 with permission from Oxford University Press, copyright 2017. (H) PET images of an AD human brain acquired with $^{18}$F-PI-2620 exhibit a high contrast and signal-to-noise ratio. Reproduced from ref. 53 with permission from SNMMI, copyright 2020.

transfer and marked fluorescence response selectively in the presence of tau aggregates over Aβ. Molecular docking with VQIVYK revealed that Q-tau-4 interacts with the hydrophobic surface of Gln307 along the fibril axis. Further *ex vivo* staining of the AD brain tissue with Q-tau 4 reveals its selective colocalisation with tau protein antibodies over Aβ (Fig. 3D and E). Most of the probes developed target tau aggregates and there are limited probes targeting tau oligomers and soluble tau aggregates, which are believed to have more disease relevance. A thiophene-based ligand pTP-TFE shows turn-on fluorescence upon interaction with soluble tau aggregates, and strongly binds to tau oligomers with a $K_d$ of 66 nM.[48] The probe is biocompatible, cell-permeable, and successfully stains early tau aggregates in the AD and PSP human brain sections.

**Tau PET and MR imaging.** Arylquinoline based PET probes $^{18}$F-THK5117 and $^{18}$F-THK5351 have emerged with superior *in vivo* imaging characteristics with $^{18}$F-THK5117 being better than $^{18}$F-THK5351 (Fig. 3F).[49] A novel PET probe flortaucipir ($^{18}$F-AV-1451, Tauvid) from an indole moiety was developed for imaging tau aggregates (Fig. 3F).[50] Clinical investigations demonstrated the good brain uptake, selective labelling of tau aggregates, and safety of flortaucipir, which received FDA approval for clinical use for AD diagnosis (Fig. 3G). In a preclinical evaluation, another probe $^{18}$F-JNJ64349311 was superior to Tauvid.[51] Genentech has developed a PET probe $^{18}$F-GTP1 that overcomes the off-target interactions with Aβ and monoamine oxidase (MAO).[52] Another probe $^{18}$F-PI-2620 in the human clinical trial has shown excellent imaging features with a high contrast, signal-to-noise ratio, and selectivity that accurately distinguish AD from healthy controls (Fig. 3H).[53] The tau deposition pattern with $^{18}$F-PI-2620 also correlates with cognitive performance and possesses high diagnostic potential.

The availability of MRI probes targeting tau pathology are limited, and recently few probes are developed and evaluated in Tg mouse models. A novel buta-1,3-diene derived $^{19}$F-MRI probe Shiga-X35 was developed targeting tau tangles for MR imaging.[54] *Ex vivo* immunofluorescence and *in vivo* $^{19}$F-MR imaging in a rTg4510 mouse model revealed that Shiga-X35 colocalises with tau tangles and accumulates in the forebrain of the Tg AD mouse. The *in vivo* $^{19}$F-MRI signal from the AD mouse brain was significantly higher which distinguishes AD from the WT mouse. The accumulation of hyperphosphorylated tau inside the neuronal cells is an early event of tau pathology in AD that possibly changes the cell surface markers. In this context, an aptamer-based nanoparticle MRI contrast agent tau-X targeting the neurons with hyperphosphorylated tau was developed for evaluating tau pathology by MRI.[55] An aptamer that selectively binds to the neuronal cells with intracellular hyperphosphorylated tau was evolved by systematic evolution of ligands by the exponential enrichment (SELEX) method. A lipid nanoformulation tau-X was prepared using the aptamer and Gd-DOTA contrast agent. The developed tau-X MRI agent was evaluated in a 2 month old P301S Tg mouse model and age matched control, which showed a higher MRI signal in the AD mouse that developed tau accumulation compared to WT. Recently, improved aptamers were evolved and prepared tau-X nanoformulation, and evaluated for their MRI in a Tg mouse model.[56] The results showed that tau-X based MRI successfully detects tau pathology in an early stage (2 months) in the Tg mouse model and may have implications for early detection of tau pathology in clinical cases.

### 2.4 Neurodegeneration (N)

The correlation of neurodegeneration with cognitive decline, Aβ, and tau made it one of the reliable biomarkers in the ATN framework. The assessment of brain metabolism and atrophy is performed by PET and MR imaging. In a multicentric study, fluorodeoxyglucose–PET ($^{18}$FDG–PET) was employed to measure brain metabolism as a biomarker in AD and other dementia cases.[57] The standardised signal pattern for each disease was developed and the PET scans diagnosed AD with 95% accuracy and differentiate from mild cognitive impairment (MCI) and other dementia cases *viz.*, dementia with Lewy bodies (DLB), frontotemporal dementia (FTD) and normal individuals. Meta-analysis has suggested that FDG–PET can diagnose AD with 91% sensitivity and 78% specificity.[58] Recently, in a large clinical study FDG–PET imaging was employed on amyloid and tau positive (A+T+) patients to evaluate the ability of FDG–PET for AD diagnosis.[59] Study revealed that FDG–PET (F+) has differentiated AD from dementia and suggests F+ as an independent biomarker for AD. FDG–PET was considered for differential diagnosis of AD from other forms of dementia and the output is inconsistent and needs to be revisited before recommending it for AD diagnosis.[60] There is a need for developing robust artificial intelligence (AI) and machine learning approaches for defining the patterns of brain hypometabolism for differential diagnosis of dementia.

Structural MR imaging assesses brain tissue damage and atrophy evident in AD. Brain regiospecific volume measurements by MRI scans revealed volume reduction in various regions of the AD brain compared to healthy controls and the changes track the progression of AD.[61] The brain volumetric measurements carried out using MRI of MCI in a longitudinal study demonstrate that MCI cases converted to AD had lower volumes compared to controls.[62] The analysis of atrophy in the brains of DLB, AD, and controls by MRI demonstrates the bilateral damage of cornu ammonis and subiculum in AD, whereas it was intact in DBL.[63] The study showed the ability of structural MRI for differential diagnosis and its potential application in other neurodegenerative disorders. Loss in neuronal function and degeneration was expected to affect the functional connectivity within the AD brain. The characterisation of brain network alterations by functional MRI in MCI and AD with disease progression in the longitudinal study suggests a gradual decline in the functional networks of AD compared to healthy controls.[64] Studies have found that the connectivity alterations are specific to the disease and need to be characterized for accurate discrimination. A recent study by resting-state functional magnetic resonance imaging (rs-fMRI) revealed a decline in the connectivity between the posterior cingulate cortex to the whole brain for AD subjects.[65] The functional connectivity changes need detailed characterization in the AD brain to use as a diagnostic marker.

### 2.5 Indirect biomarkers

Complex etiopathologies associated with AD were unrevealed in the last decade and many pathological events occur in preclinical stages. Oxidative stress, neuroinflammation, and synaptic damage are among the major early events and there are many associated biomolecules and biomolecular events that indirectly influence AD pathology, which are considered potential indirect biomarkers for AD diagnosis. These indirect biomarkers are promising, and their identification and validation may find a place in the NIA-AA framework along with ATN as additional biomarkers for early and accurate diagnosis.

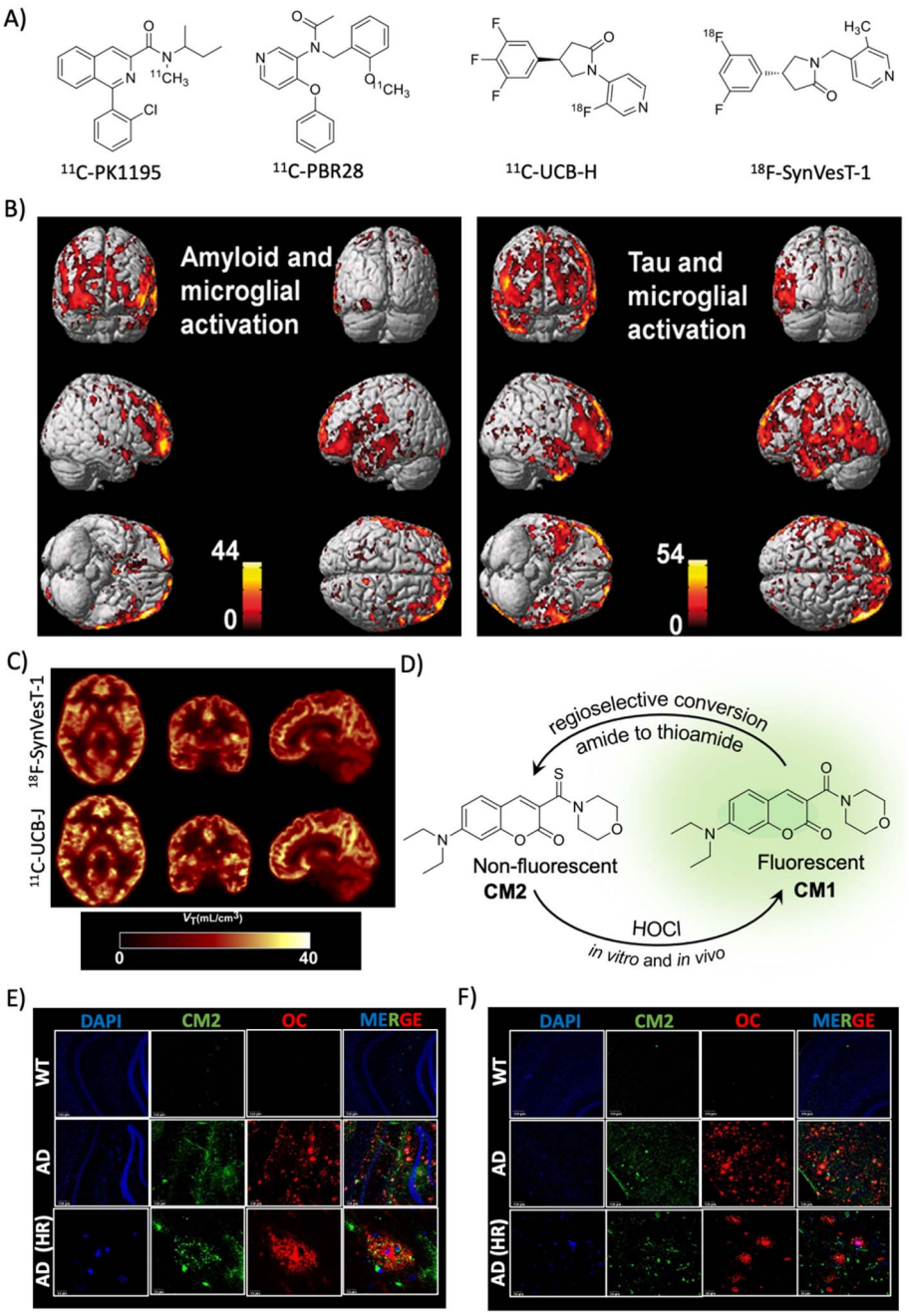


Fig. 4 Targeting indirect biomarkers of potential diagnostic importance. (A) PET probes targeting TSPO and SV2A. (B) PET imaging of microglial activation in the AD human brain using the PBR28 probe. The accumulation of the probe in the brain correlates with Aβ and tau deposition as revealed by PET imaging. Reproduced from ref. 68 with permission from Oxford University Press, copyright 2018. (C) PET imaging of synaptic density in the AD brain targeting SV2A protein using $^{18}$F-SynVesT-1 and $^{11}$C-UCB-J. Reproduced from ref. 71 with permission from SNMMI, copyright 2020. (D) Regioselective conversion of a non-fluorescent CM2 probe to fluorescent CM1 in the presence of HOCl under *in vitro* and *in vivo* conditions. Elevated levels of HOCl proximally localised with Aβ aggregates (OC) detected by the CM2 probe in the cortex (E) and hippocampus (F) of the APP/PSEN1 Tg AD mice brain (scale bar 20 μm). Reproduced from ref. 73 with permission from the American Chemical Society, copyright 2019.

**Microglial activation.** Microglial cells are activated in the AD brain and translocator protein 18 kDa (TSPO), a small mitochondrion protein, is an indicator of microglial activation. The TSPO levels increased significantly in AD and many probes are developed to image TSPO *in vitro* and *in vivo* due to its potential implication as a biomarker for AD and other CNS disorders (Fig. 4A).[66] In a clinical study, AD and MCI subjects (42) were assessed for TSPO using $^{11}$C-PK11195 and found evidence of microglial activation as an early event in MCI and a strong correlation with Aβ load (PiB).[67] In an attempt to understand the correlation of microglial activation with Aβ and tau aggregate accumulation, PET imaging was performed for three markers in 52 MCI subjects.[68] The results showed that TSPO imaged with $^{11}$C-PBR28 has a good correlation with Aβ and tau accumulation in both MCI and AD cases with TSPO mapping overlapping with Aβ deposition (Fig. 4B).

**Synaptic density measurement.** In AD, there is synaptic damage and a decline in the synaptic density, and two relevant markers of synaptic integrity are synaptophysin and synaptic vesicle glycoprotein (SV2A) and serve as potential diagnostic biomarkers. SV2A is a vesicular glycoprotein specifically expressed in synapse and used as a measure of synaptic density. It is involved in neurotransmission and other biomolecular transportation. PET probes binding to SV2A protein effectively measured the synaptic density and distinguish AD subjects from healthy individuals. Levetiracetam is a drug developed for epilepsy and bind to SV2A, which was further subjected to structural modification and radiolabelling to generate PET probes (UCB-A, UCB-H, and UCB-J) with enhanced target affinity. The first *in vivo* synaptic density was imaged in human subjects targeting SV2A using $^{11}$C-UCB-J (Fig. 4A).[69] SV2A imaging using $^{11}$C-UCB-J was successful in the quantification of synaptic loss in patients of temporal lobe epilepsy. The synaptic loss in AD was probed with another probe $^{19}$F-UCB-H targeting SV2A (Fig. 4A).[70] The imaging data suggest the reduction of synaptic density in the hippocampus and a few areas of the cortex in AD compared to age-matched healthy individuals, which correlates with cognitive impairment and Aβ load. $^{11}$C-UCB-J has been modified into a difluoro analogue $^{18}$F-SynVesT-1 and used in primate studies and human trials, which revealed favourable kinetics and binding properties with the ability to measure the synaptic density (Fig. 4C).[71] Another PET probe $^{18}$F-SynVesT-2 was also assessed in humans and showed high brain uptake, fast kinetics, and specific binding to SV2S.[72] These two PET probes are promising for clinical use, and need to be evaluated for their practical utility for AD diagnosis.

**Combination biomarkers.** An elevated level of ROS and oxidative stress is evident in the AD brain.[6] Myeloperoxidase converts $H_2O_2$ into HOCl in the presence of chloride and possibly in AD the HOCl level is altered. We have developed a coumarin–morpholine (CM2) conjugate probe as a turn-on fluorescent probe for HOCl detection.[73] The designed non-fluorescent thioamide probe (CM2) undergoes regioselective transformation to a fluorescent amide (CM1) by HOCl (Fig. 4D). The probe is highly selective among different ROSs and shows a turn-on response with 90-fold fluorescence enhancement (quantum yield from null to 0.32) with a limit of detection (LOD) of 0.17 μM. The probe is biocompatible, crosses BBB, and detects HOCl in cells and mouse brain tissue. The probe has unambiguously detected elevated levels of HOCl in the Tg APP/PSEN1 mouse model and immunostaining with Aβ antibodies (OC) revealed that HOCl is produced and proximally localised with Aβ plaques (Fig. 4E and F). This molecular probing suggests that HOCl is associated with Aβ plaques and serves as a potential combination biomarker for AD diagnosis.

**Metal ion detection.** Post-mortem AD brain studies have revealed an abnormal increase in the levels of biometals copper (Cu), zinc (Zn) and iron (Fe) (5.7, 3.1 and 2.8 fold, respectively, compare to healthy controls) and significant levels of aluminium (Al) in the AD brain compared to healthy controls.[74,75] The accumulation and dyshomeostasis of these metal ions in the brain have diagnostic implications. Fe is a good contrast agent for MRI and elevated levels serve as a diagnostic marker. A recent study demonstrated MRI scanning of regiospecific accumulation of Fe for AD diagnosis.[76] The Fe level was higher in the gray matter and neocortical region of the AD brains compared to healthy controls reflecting its diagnostic value. Studies by PET imaging have demonstrated altered copper trafficking in the Tg AD mouse model highlighting the possible role of copper levels in AD diagnosis.[77–79] Higher levels of Zn and Al in the brain influence the disease pathology and their measurements in the brain are a potential biomarker.[74,84–88] There are many chemical tools developed to selectively detect and image metal ions that could be exploited to assess the metal ion levels in the AD brain for diagnosis.[78–88] We have developed selective fluorescence sensors for the detection of copper and iron, and evaluated *in vitro* and cell models.[78,79,82,84] A dual response colorimetric and fluorescence sensor for the differential detection of Zn and Al and fluorescence sensors for Zn and Al were developed.[81,83,85] Kim and co-workers developed a selective and sensitive fluorescent off-on sensor for Zn and evaluated *in vitro* and *in vivo* cell and animal models.[86,87] They recently developed a colorimetric and fluorescent dual responsive chemical probe for bioimaging of Fe in cells.[88] The reported chemical probes are demonstrated for *in vitro* and *in vivo* applications. These probes need to be explored for their utility in the diagnosis of AD by the detection and imaging of biometals in the clinical context.

### 2.6 Circulating biomarkers

Imaging the pathological lesions in the brain encounters limitations of exposure to radiation, complicated procedures, instrumentations, and the need for clinical experts. Disease associated alterations in the brain are expected to be reflected in the circulating fluids like CSF and blood. These circulating biomarkers have the advantage of being minimally invasive or non-invasive, simple, and cost-effective. In recent years, circulating biomarkers have been explored and potential biomarkers are identified for early and accurate diagnosis of AD (Fig. 5 and Table 2).[89,90] Many biomarkers associated with AD pathology are altered in CSF and blood in the early stage, and correlate with

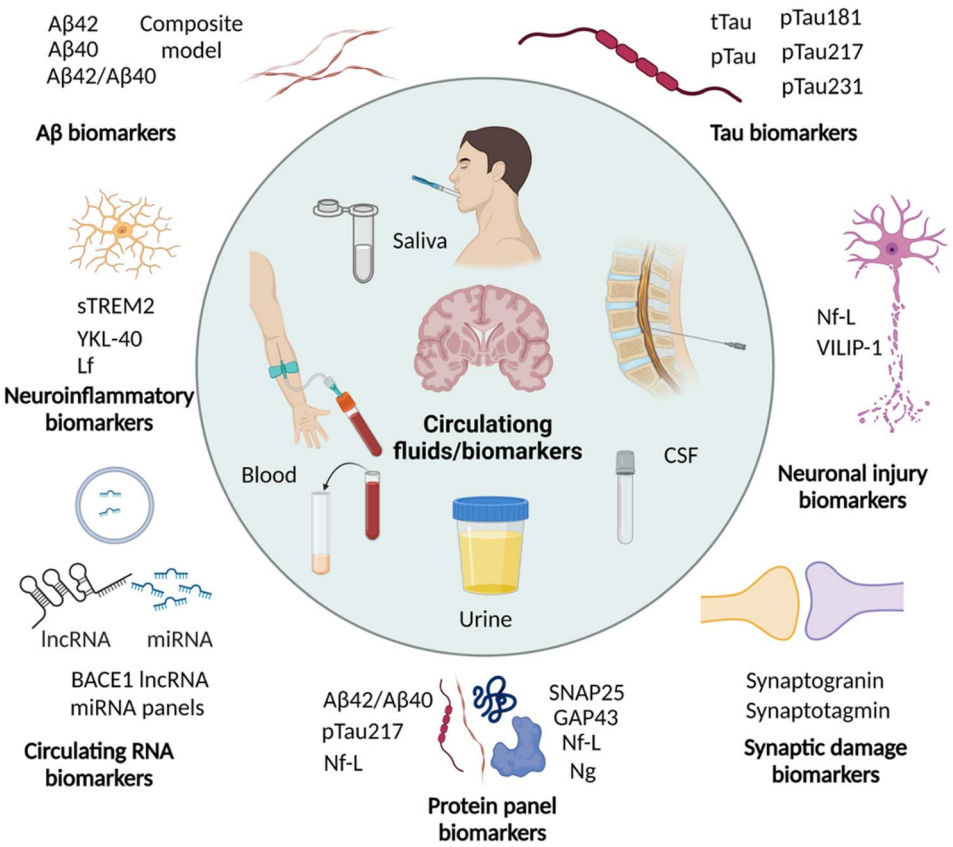


Fig. 5 Circulating biomarkers in CSF, blood, saliva, and urine for the diagnosis of AD (created with BioRender.com).

ATN and cognitive decline. Due to non-invasiveness saliva and urine are also explored and their potential is yet to be proven.

**Aβ and tau biomarkers in CSF and blood.** In a clinical study, decreased plasma Aβ42 and Aβ42/Aβ40 were evident in Aβ PET (PiB) confirmed AD subjects.[91] The decreased Aβ42/Aβ40 ratio well correlates with disease and diagnoses with 84% sensitivity and 100% specificity. A multicentric clinical study of a large sample size was conducted in Japan and Australia to assess Aβ peptides in plasma by a sensitive immunoprecipitation coupled with mass spectrometry (MS) technique in Aβ PET confirmed cases.[92] They have developed a mathematical model based on Aβ42, Aβ40, and ratio changes and the model successfully discriminates MCI, AD, and healthy controls and diagnoses AD with 90% accuracy, 96.7% sensitivity, and 81% specificity. In another study, the diagnostic utility of the plasma Aβ ratio complemented with FDG–PET was evaluated in PiB confirmed AD cases.[93] The results revealed that the Aβ42/Aβ40 ratio independently discriminates AD from healthy controls. Further attention and efforts are necessary to improve the sensitivity with advanced methods and techniques.

The pathological phosphorylation of tau (p-tau) is evident in AD and p-tau variants are anticipated to serve as biomarkers for diagnosis. A recent study has shown significantly elevated levels of CSF tau, CSF pTau, and plasma tau in AD compared to healthy controls.[94] A large cohort study of p-tau-181 in CSF and plasma demonstrated high levels in preclinical dementia cases, which further increased in MCI and AD.[95] The plasma level of p-tau-181 was correlated with CSF levels and tau PET positivity, and accurately differentiate dementia cases of non-AD subjects, MCI, and AD. A recent cohort study to analyse p-tau isoforms in CSF by the sensitive MS technique demonstrated that the CSF p-tau-217 isoform outperforms p-tau-181 for the diagnosis of PET confirmed AD cases.[96] It was supported by another cohort and longitudinal study and demonstrated that p-tau-217 levels strongly correlate with tau and Aβ PET results and accurately diagnose AD and distinguish it from other dementia. The analysis of plasma p-tau levels in the cohorts of Aβ and tau PET confirmed preclinical and prodromal AD cases, and there was an association of plasma p-tau-217 with CSF p-tau-217 levels and tau PET positivity.[97] Plasma and CSF p-tau-217 have increased significantly in the early stage of disease, wherein tau and Aβ deposition was not significant. These observations suggest p-tau-217 as one of the potential biomarkers for early diagnosis. In a retrospective study, plasma p-tau-181 and p-tau-217 showed excellent diagnostic performance and distinguish AD from other disease conditions.[98] Recently p-tau-231 has emerged as a potential blood biomarker for early and accurate diagnosis of AD.[99] The increased p-tau-231 distinguishes MCI and AD from healthy individuals outperforming p-tau-181 and correlates with Aβ and tau deposition. These circulating p-tau isoforms hold high diagnostic potential that needs to be established by multicentric longitudinal and cross-sectional clinical studies with large cohorts.

**Synaptic damage, neuroinflammation and neuronal injury biomarkers in CSF and blood.** The synaptic damage in neurons was evident in AD and an altered level of postsynaptic protein neurogranin was observed in synaptic damage and loss. The diagnostic potential of CSF neurogranin was assessed in a cross-sectional and longitudinal study, which revealed elevated levels in AD compared to healthy controls.[100] The increased CSF neurogranin levels correlate with other CSF markers (Aβ and tau), brain atrophy, Aβ load, and cognitive decline that serve as an early preclinical AD biomarker. Recently, a study contradicting the previous studies of neurogranin as a diagnostic marker reported that neurogranin fails to differentially diagnose AD.[101] The analysis of CSF synaptotagmin, another synaptic marker, by the MS-based approach showed significantly increased levels in MCI and AD cases, which demonstrates the ability to discriminate both these clinical conditions.[102] In a longitudinal clinical study, the analysis of a soluble triggering receptor expressed on myeloid cells 2 (sTREM2, a microglial marker) changes in CSF and its association with other biomarkers demonstrates its diagnostic ability in autosomal dominant AD cases.[103] Increased sTREM2 levels in CSF correlate with decreased Aβ42 in CSF, Aβ deposition in the brain and atrophy. YKL-40 is known to be altered in the AD brain, which is expected to be reflected in circulating fluids and possibly serve as a biomarker. The analysis of plasma YKL-40 levels with other AD biomarkers revealed a negative and positive correlation with Aβ deposition and memory performance, respectively.[104] Increased YKL-40 levels in serum effectively differentiate dementia cases from healthy cases with 85% specificity and sensitivity outperforming total tau (t-tau).[105] Neurofilament light chain (Nf-L) is a protein marker for neuronal injury in CNS disorders. The longitudinal assessment of Nf-L levels showed a peak level at the stage of conversion from non-symptomatic to symptomatic AD and correlates strongly with brain atrophy, and moderately with Aβ deposition and glucose metabolism, which suggests Nf-L as a biomarker to assess the progression of neurodegeneration.[106] In another multicentric study, it was evident that plasma Nf-L levels were significantly elevated and distinguished dementia cases from healthy controls.[107] Nf-L fails to differentially diagnose different disease conditions while relatively higher levels are observed in Parkinson's disease (PD). The CSF levels of visinin-like protein 1 (VILIP-1), a calcium sensor protein, and other AD biomarkers were analysed and compared.[108] VILIP-1 measurement successfully diagnoses MCI and AD from healthy controls and correlates with other standard biomarkers. Thus, VILIP-1 with other biomarkers can serve as a diagnostic and prognostic marker, as evident from the correlation with cognitive decline.

**Circulating RNA biomarkers.** Non-coding RNAs (ncRNAs) have a potential role in the pathogenesis of AD and there is limited evidence of ncRNAs as a diagnostic marker. In the last decade, circulating RNAs were explored as diagnostic biomarkers. The analysis of four long noncoding RNAs (lncRNAs) associated with AD in plasma revealed that BACE1 lncRNA levels significantly increased in AD compared to control and change was specific to AD.[109] Exosomes are the carriers of microRNA (miRNA) from the brain to peripheral circulation. The miRNA in the exosome enriched plasma was assessed in AD and healthy controls and significant alteration of 20 miRNA levels was found.[110] A machine learning model was developed considering seven altered miRNAs that diagnose AD with 89% accuracy. The analysis of 179 miRNA levels in the plasma of MCI, AD and control plasma samples by commercially available RT-PCR assays found that 26 miRNA levels are altered that regulate the mRNA of proteins associated with different pathological pathways of AD.[111] Further analysis of 15 promising miRNAs linked to AD revealed 6 miRNAs that diagnose AD from control individuals suggesting their diagnostic potential. The assessment of 37 miRNAs associated with AD in CSF for the validation of their diagnostic potential revealed that 26 miRNAs hold potential.[112] The altered levels of miRNA correlate with CSF markers (Aβ42 and t-tau) and cognitive scores (MMES). Among them, a 7 miRNA panel identified the AD subjects from the control and these miRNA panels along with CSF biomarkers significantly enhance the diagnostic performance.

**Protein and metabolite panel biomarkers.** Protein analysis in plasma samples of AD cases identified a panel of proteins dysregulated that distinguish MCI from AD and diagnose with high sensitivity and specificity.[113] A recent study showed that the plasma Aβ42/40 ratio, p-tau-217, and Nf-L together can accurately predict the progression of AD and correlates with cognitive decline.[114] The analysis of CSF proteins revealed the association of synaptic marker neurogranin, growth-associated protein-43 (GAP-43), synaptosomal-associated protein-25 (SNAP-25), and synaptotagmin-1 with increased deposition of Aβ and the changes in synaptic markers were evident in the early stage.[115] The identified synaptic markers in CSF are promising in early diagnosis of AD and monitoring disease progression. Blood exosomal protein was analysed to develop synaptic markers and it was found that growth associated protein43 (GAP43), neurogranin, synaptosome associated protein 25 (SNAP25), and synaptotagmin-1 levels were reduced in AD compared to controls.[116] Similarly, blood metabolite analysis revealed a panel of sphingomyelin metabolites associated with AD, which are used as biomarkers for the diagnosis and prognosis of AD.[117] Thus, the panel of proteins and metabolites may aid in early and accurate diagnosis of AD in the near future.

**Biomarkers in other fluids: saliva, urine and tears.** Saliva is a composite biofluid that contains several proteins and metabolites that reflect the physiological conditions of the body and its composition can be potentially disturbed under disease conditions. In a clinical study, Aβ biomarker analysis showed significantly higher salivary Aβ42 levels in AD subjects.[118] Similarly, the analysis of tau biomarkers in saliva showed an increased p-tau/t-tau ratio in AD compared to control subjects, which emphasise its diagnostic potential.[119] A recent analysis of different isoforms of tau demonstrated increased levels of a specific isoform p-tau-396/t-tau in AD.[120] However, there was a large variation in the levels and did not correlate with CSF biomarkers and brain atrophy. In a cross-sectional study, the lactoferrin (Lf) level was significantly decreased in MCI and AD cases compared to control individuals and discriminate MCI

and AD.[121,122] This finding was contradicted by a recent study, which showed no significant difference in the CSF and salivary Lf levels between mixed dementia cases and the control group.[123] The diagnostic ability of Lf has to be further evaluated and proven to establish it as a reliable circulating biomarker. Global protein composition analysis of tears from AD cases shows increased total protein concentration and combinations of four proteins (lipocalin-1, dermcidin, lysozyme-C and lacritin) identify AD with 81% sensitivity and 77% specificity.[124] The analysis of urine using a MS-based technique identified exclusively high levels of 15 proteins in urine samples of AD compared to healthy controls.[125] Further validation with enzyme-linked immunosorbent assay (ELISA) showed differential expression of secreted phosphoprotein 1 (SPP1), gelsolin (GSN), and insulin-like growth factor-binding protein 7 (IGFBP7), which may have diagnostic potential.

### 2.7 Multiplexing and multimodal diagnosis – a future approach for AD diagnosis

Chemical tools for NIRF, PET, and MR imaging targeting different core and indirect biomarkers have been established for the diagnosis of AD. Each of these tools and techniques holds merits and limitations. Developing chemical probes for multimodal imaging overcomes the limitations and enhances the sensitivity, specificity, and resolution of imaging that aids the accurate diagnosis of AD. Simultaneous detection of multiple diagnostic biomarkers by multiplexing is another approach to improve the accuracy and reliability of diagnosis. Multiplexed detection of Aβ, tau, and neurodegeneration by multimodal imaging using different probes targeting multiple biomarkers or with a single probe targeting different biomarkers is anticipated to gain utmost importance soon (Fig. 6).[14,126] Multiplexed detection of multiple circulating biomarkers using multiple assays or integrated microarrays can be considered as the future direction for research on AD diagnostics. Protein, RNA, and metabolite biomarkers in circulating fluids can be detected by multiplexing with different modes of detection like MS, ELISA, microarrays, and paper-based sensors. In general, the detection of multiple biomarkers with multiplexed and multimodal approaches to develop the signature fingerprint is the future of AD diagnostics (Fig. 6).[14,126] Such characteristic fingerprints hold potential for early diagnosis and accurate categorisation of clinical stages for better management and personalised detection and medication for AD patients.

## 3. Therapeutic strategies

### 3.1 AChE and *N*-methyl-D-aspartate (NMDA) receptor targeted therapies

AD drug discovery initially focused on the amyloid pathway and cholinergic deficiency as therapeutic targets. The efforts were made to target acetylcholine esterase (AChE) to improve the acetylcholine (ACh) levels and restore neuronal function. NMDA receptor signalling is involved in brain activity and abnormal brain activity is evident in AD. NMDA receptor antagonists were developed to overcome the abnormal brain activity that restores learning and memory functions. AChE acts in the synapse to cleave ACh into acetate and choline, and inhibition of the enzyme was expected to increase ACh levels in synapse and improve memory deficits (Fig. 7A). In this direction many AChE inhibitors have been developed and assessed in preclinical and clinical trials for therapeutic effects.[127] Among the approved

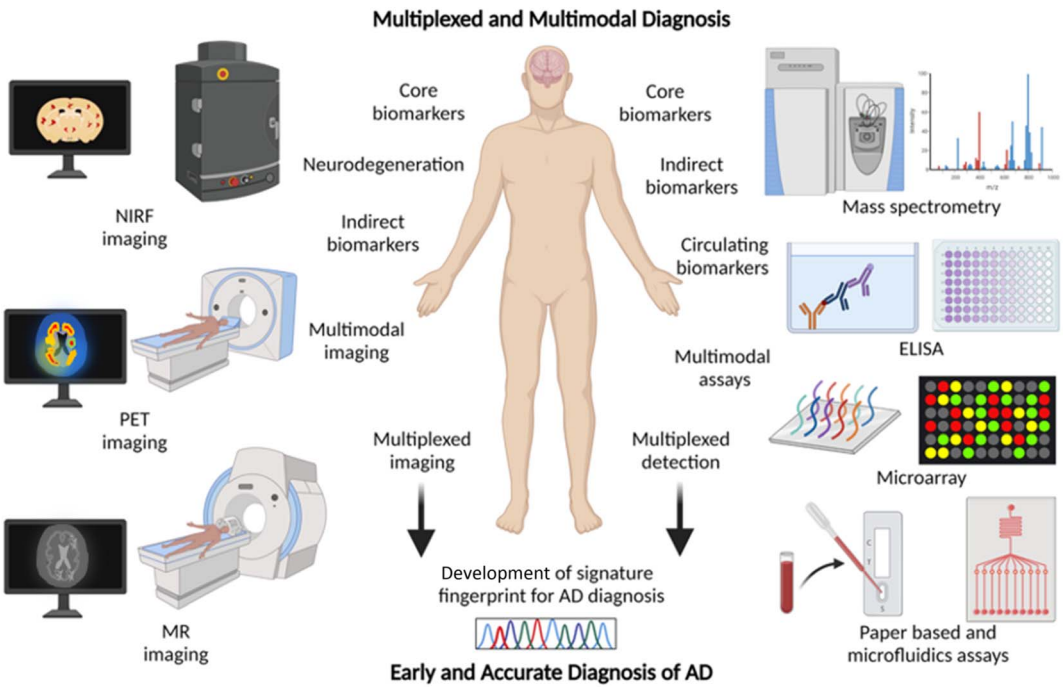


Fig. 6 Multiplexing and multimodal approach for early and accurate diagnosis of AD (created with BioRender.com).

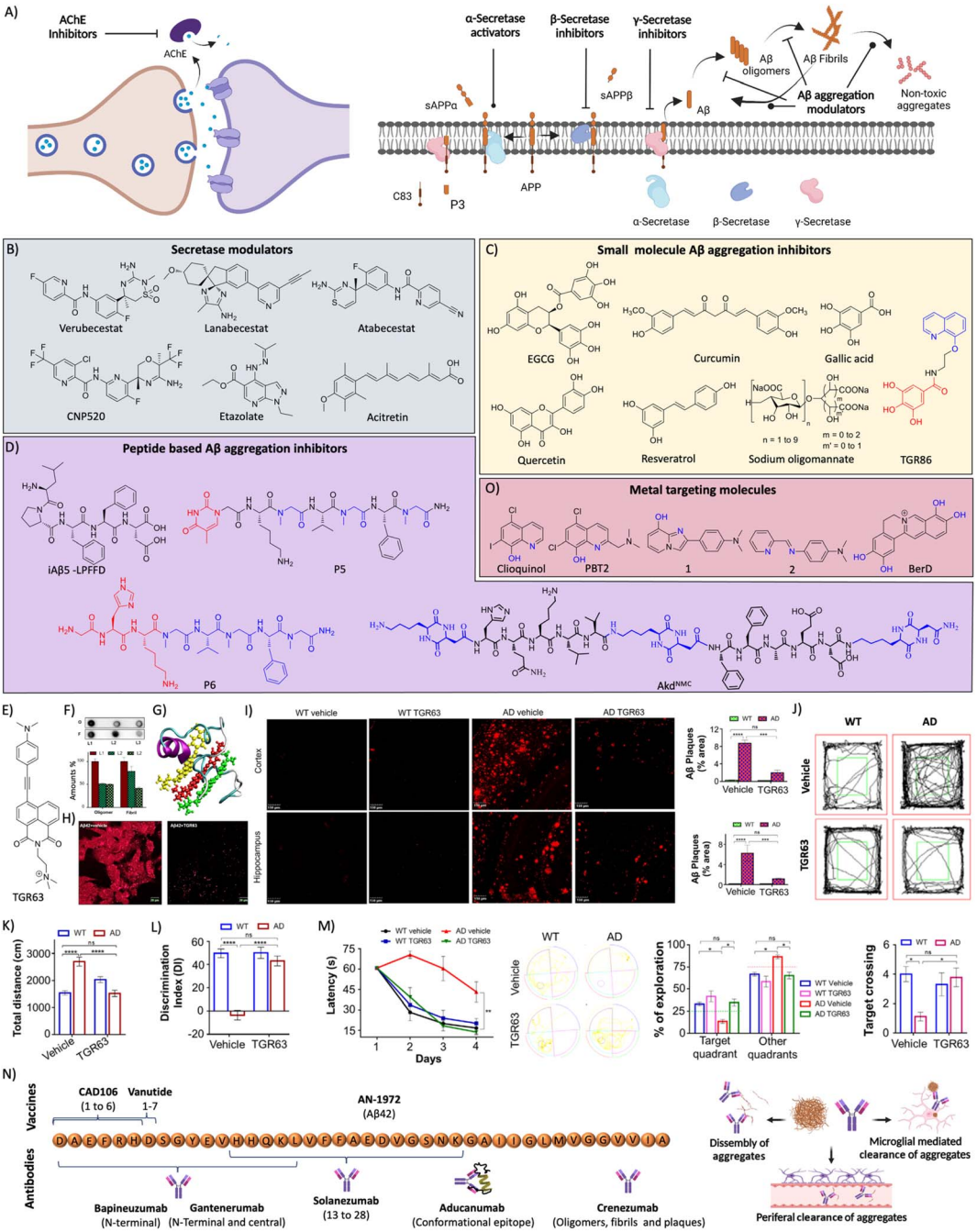


Fig. 7 (A) Therapeutic approaches to target cholinergic and amyloid pathways. Therapeutics targeting (B) secretases, and (C) small molecules for Aβ aggregation (blue: quinoline moiety from clioquinol and red: phenolic moiety from EGCG in TGR86). (D) Peptides and peptidomimetics for Aβ aggregation (blue: sarcosine moiety and red: thymine in P5; blue: hybrid peptoid and red: GHK tripeptide in P6; blue: cyclic dipeptide kd in $Akd^{NMC}$). (E) Chemical structure of TGR63. (F) Dot blot assay of Aβ oligomer and fibril inhibition by TGR63 and its quantification in the absence (L1) and presence of TGR63 at two different molar ratios 1 : 1 (L2) and 1 : 5 (L3). (G) Binding of TGR63 with Aβ42 by MD simulation. (H) Reduction of the membrane toxicity of Aβ fibrils by TGR63 revealed by immunofluorescence with fibril antibodies. (I) Immunofluorescence images show the amelioration of amyloid load in the APP/PSEN1 Tg mice model with the treatment of TGR63 and its quantification. (J) Tracing of control and TGR63 treated mice in an open field test and (K) quantification of the total distance travelled by subjects. (L) Novel object recognition by control and treated animals as a measure of the discrimination index (DI). (M) TGR63 treatment rescue learning and memory deficits as revealed by improvement in the latency period, exploration and target crossing from the MWM test. (N) Schematic representation of fragments for Aβ vaccines, the target site of mAb and mechanism of action of mAb in Aβ reduction. (O) Therapeutics targeting metal ion toxicity (blue: metal binding moiety). (F)–(M) Reproduced from ref. 150 with permission from Wiley-VCH, copyright 2021.

candidates for AD treatment mostly they are AChE inhibitors like tacrine, donepezil, rivastigmine, and galantamine.[128] Another approach of counteracting the cholinergic deficiency is to treat with cholinergic precursors like choline or choline alphoscerate that stimulate the cholinergic system. The association between the cholinergic precursors and AChE inhibitors

results in effective combination treatment. The treatment of rats with rivastigmine in association with choline or choline alphoscerate increased ACh levels, inhibited AChE and restored cholinergic transmission.[129] In a double blinded clinical trial, donepezil and choline alphoscerate treated AD patients with ischemia showed improvements in behavioural and cognitive functions compared to control and donepezil treated patients.[130] In a recent clinical study, AD patients treated with donepezil and choline alphoscerate showed improvement of depression symptoms.[131] Cholinergic stimulation with donepezil along with a cholinergic precursor choline alphoscerate was effective in mild to moderate AD cases. Many NMDA receptor antagonists were developed and among them memantine was beneficial and approved for clinical use. They all are proven to improve the clinical conditions of AD but fail to address the root cause and cure the disease. They were tried in combination with many other drugs and analogues are in assessment for therapeutic benefits.

### 3.2 Aβ targeted therapies

Aβ peptide is generated from amyloid precursor protein (APP) by enzymatic cleavage of β- and γ-secretase through the amyloidogenic pathway. The action of α-secretase and γ-secretase follows the non-amyloidogenic pathway that generates physiologically non-toxic peptides. Amyloidogenic processing results in the generation of Aβ peptides that misfold and aggregate to form toxic oligomers, protofibrils, and fibrils. Amyloid-targeted drugs were developed to modulate secretase enzymes and Aβ aggregation (Fig. 7A).

**Secretase modulators.** The inhibition of β-secretase (BACE1) was directly targeted to inhibit the production of Aβ peptide (Fig. 7B). Several small molecule inhibitors have been developed over the last two decades and many reached clinical trials with limited success. Verubecestat (MK-8931), lanabecestat (subnanomolar $IC_{50}$), and atabecestat were developed as BACE1 inhibitors and they displayed therapeutic benefits in preclinical and phase 1/2 clinical trials.[132] They failed to exhibit therapeutic efficacy in phase 2/3 clinical trials and terminated due to side effects. Umibecestat (CNP520) was recently developed as a selective BACE1 inhibitor that was long-acting and reduced Aβ in CSF and the brain of rats.[133] Clinical studies showed that the compound was safe and exhibits a dose-dependent effect. γ-secretase is another counterpart that processes APP and also possesses other physiological importance (notch protein signalling). There were attempts to develop γ-secretase inhibitors that were tested in various clinical stages, which mostly encountered toxicity issues and were discontinued.[134] Attempts need to be directed towards the development of drug candidates with high potency and selectivity towards γ-secretase and avoid the off-targets like notch to evolve better therapeutics. Failures of BACE1 and γ-secretase inhibitors emphasise the need for an alternate approach that could improve the Aβ targeting therapies (Fig. 7B). Etazolate (EHT-0202) is one of the compounds developed to activate the α-secretase and the gamma-aminobutyric acid (GABA) receptor.[135] The compound was safe to treat in AD cases but there was no significant improvement in the memory score. Acitretin is a synthetic vitamin-A derivative that activates α-secretase and enhances the non-amyloidogenic APP processing. An initial clinical study revealed the safety and activation effect as evident in the elevated CSF sAPP levels and reduction in the Aβ levels.[136] A potent α-secretase activator APH-1105 in nanoparticle formulation was developed as an intranasal treatment and is in a clinical trial. The safety and efficacy assessed in the phase 2 clinical trial would infer the potential of the drug candidate in the near future (NCT03806478).[137]

**Aβ aggregation modulators.** Aβ, an amyloidogenic peptide aggregate to form toxic species, results in disease pathology. The molecules that interact with Aβ and inhibit the aggregation have been explored as a potential therapeutic strategy (Fig. 7C). In this context, polyphenolic and other natural compounds such as epigallocatechin gallate (EGCG), curcumin, gallic acid, quercetin, resveratrol, and myricetin among others have been assessed for their Aβ aggregation inhibition ability and found effective. Polyphenols owing to their antioxidant activity and other beneficial effects exhibit therapeutic benefits in preclinical and early clinical studies but failed in later stages. Sodium oligomannate derived from marine algae has been shown to inhibit the Aβ aggregation and restore healthy gut microbiota.[138] It has been approved to treat AD cases in China and is under clinical trial to further evaluate safety and efficacy (NCT02293915). Gut microbial dysbiosis has pathological implications through the gut–brain axis and is considered a potential therapeutic target.[139] Multifunctional molecules were designed by conjugating a clioquinol (Clq) moiety for metal chelation and a polyphenolic moiety from EGCG as an antioxidant module to develop an Aβ aggregation modulator TGC86 that effectively inhibits amyloid aggregation and mitochondrial damage (Fig. 7C).[140] Peptide-based molecules were designed for anti-aggregation properties and inhibit the fibrillogenesis (Fig. 7D). Soto *et al.* designed and evaluated 5 residues iAβ5 peptide that inhibited Aβ aggregation and dissolved fibrils *in vitro* and *in vivo*.[141] The core recognition sequence of Aβ inspired the development of peptide-based inhibitors of its fibrillogenesis.[4,142] Alanine substitution studies demonstrated that Lys16, Leu17 and Phe20 residues are essential for binding to Aβ peptide. We have rationally designed peptidomimetics (hybrid peptoids) derived from the KLVFF peptide to overcome the limitations like serum stability and enhanced Aβ42 interaction by incorporating moieties with multiple hydrogen bonding donor–acceptors (thymine/barbiturate) and sarcosine at alternative positions.[143] Among designed peptidomimetics, P4 and P5 inhibit Aβ aggregation and dissolve preformed aggregates (Fig. 7D). The studies in an Aβ expressing *Saccharomyces cerevisiae* yeast model demonstrated the ability of hybrid peptoids to rescue cells from Aβ toxicity through the activation of autophagy. The cellular imaging data showed the dissolution of Aβ-GFP aggregates and redistribution of the dissolved monomeric species to the vacuole, which is an indication of aggrephagy to clear Aβ and rescuing of cells. Furthermore, we have designed multifunctional peptidomimetic P6 with antioxidant properties by conjugating natural tripeptide GHK of human origin for metal chelation with

 

a hybrid peptoid that modulated metal-dependent and independent Aβ aggregation and rescue neuronal cells from amyloid toxicity (Fig. 7D).[144] Ongeri and co-workers reported β-hairpin peptidomimetics containing piperidine–pyrrolidine moieties for the inhibition of Aβ aggregation.[145] Recently structure-based inhibitors of Aβ peptide aggregation were designed based on an Aβ16-26 core unit and found to be effective inhibitors.[146] We have designed peptidomimetics derived from Aβ14-23 (I) by incorporating a cyclo(Lys–Asp)-based CDP (kd) molecule at various positions to develop potent aggregation modulators with biocompatibility and stability.[147–149] The incorporation of rigid, proteolytically stable unnatural CDP amino acid (kd) with exceptional intermolecular hydrogen bonding ability overcomes the limitations of large linear and cyclic peptides. Peptides II to V were designed by incorporating Kd at the middle ($Akd^{M}$/II), C-terminal ($Akd^{C}$/III), N-terminal ($Akd^{N}$/IV), and at all three positions ($Akd^{NMC}$/V), respectively (Fig. 7D). Designer peptidomimetics II, III and V inhibit Aβ aggregation, whereas peptide IV enhanced aggregation. The lead peptidomimetic V effectively reduces ROS generation and membrane toxicity and rescues neuronal cells from Aβ toxicity. Furthermore, advanced PeakForce Quantitative NanoMechanics-Atomic Force Microscopy (PF QNM-AFM) studies using Bio-AFM have shown that peptidomimetic V effectively reduced the membrane stiffness as revealed by the decrease in abnormal stress fibers and Young's modulus. The molecular docking results revealed that incorporation of kd in the middle region close to FF residues results in strong interaction and stabilise Aβ in the monomeric state. The kd at the C-terminal and middle positions makes peptidomimetic V suitable for maximum interaction with Aβ and inhibits aggregation. This work demonstrated the utility of Aβ14-23 derived peptidomimetics for understanding and modulation of amyloid toxicity and adverse cellular mechanics, ROS and oxidative cellular stress.

Recently, we have designed a set of small molecules based on a naphthalene monoimide (NMI) core functionalised with *N*,*N*,*N*-trimethylethylenediamine as the imide substituent and electron rich *N*,*N*-dimethylamine, ethynylbenzene, and 4-ethynyl-*N*,*N*-dimethylaniline moieties to fine-tune the hydrophobicity and target Aβ.[150] *In vitro* studies demonstrated that the lead compound TGR63 has the potential to modulate Aβ aggregation and dissolve preformed aggregates (Fig. 7E and F). Further *in silico* studies to understand the mode of interaction showed TGR63 binding to surface and core binding sites mostly driven by electrostatic and van der Waals interactions. TGR63 also binds to the cryptic sites with a reduction of total hydrogen bonding and salt bridge interactions. Aβ42 fibrils consist of 81 intermolecular hydrogen bonds and 48 salt bridges that reduced to 75 and 41, respectively, in the presence of TGR63. There are two modes of binding with fibrils, core binding and surface binding. The ligand and Aβ42 fibril interaction is largely driven by electrostatic and van der Waals interactions with the latter being superior due to fact that electrostatic interactions are largely suppressed by polar solvation free energies. The interaction of TGR63 and Aβ42 monomer is mediated by three low energy binding modes (Fig. 7G). In the presence of TGR63, the α-helix content of Aβ42 effectively was reduced resulting in the formation of nontoxic globular structures. Further nuclear magnetic resonance (NMR) studies revealed the interaction of NMI and aniline aromatic protons with Aβ and the strong interaction of ethylene protons. Cellular studies showed that TGR63 rescues cells from Aβ toxicity and ameliorates membrane toxicity (Fig. 7H). Further *in vivo* studies showed that TGR63 is non-toxic (LD50 of 157.9 mg $Kg^{-1}$ BW), stable in serum (24 h), and crosses BBB. TGR63 has effectively reduced Aβ load in the AD phenotypic mice brain (APP/PSEN1 Tg mouse model) as revealed by immunofluorescence data (Fig. 7I). TGR63 rescues AD phenotypic mice from learning, memory, and cognitive deficits as revealed by different behavioural tests (Fig. 7J–M). The memory processing and explorative behavioural rescue was demonstrated by the novel object identification (NOI) test. The learning and memory improvement in TGR63 treated AD mice was observed as evident from decreased latency time and increased exploration in the target platform quadrant in the Morris water maze (MWM) test (Fig. 7M). These *in vivo* results confirmed the significant improvement in cognitive and memory deficits by TGR63 that underscore its clinical implications and is currently under consideration for further clinical studies.

**Immunotherapeutics.** Immunotherapeutics are composed of active immunisation by vaccines developed based on the peptide antigen to elicit an immune response against the target antigen and passive immunization with mAbs target pathogenic proteins. Passive immunotherapeutics with mAbs clear target proteins and aggregates by different mechanisms like dissolution, microglia-mediated removal, and clearance from the brain through circulation (Fig. 7N). AN-1972 is the first vaccine developed using Aβ42 with the QS-21 adjuvant. Immunisation in AD patients reduced Aβ load significantly without any cognitive benefits, and side effects like meningitis halted further trials.[151] Vanutide was developed by conjugating multiple short Aβ1-7 peptide sequences and was tested in a clinical trial for safety and benefits and found no therapeutic benefits.[152] CAD106 is another vaccine constructed by conjugating multiple copies of the Aβ1-6 fragment to a Qβ virus-like particle carrier. The results are promising with a safety profile with multiple doses, reduction in Aβ load and improvement in the cognitive scores.[153]

Bapineuzumab was the first mAb developed against the N-terminal of Aβ42 that selectively binds to oligomers and fibrils. A phase 3 clinical trial showed poor therapeutic effects indicating the limited success of the antibody and there is a need to look for better immunotherapeutics.[154] Solanezumab was developed targeting the Aβ13-28 segment that was safe and efficient in clearing Aβ from the brain in preclinical studies. Clinical studies revealed that antibody treatment is safe and shows dose-dependent reduction of Aβ load but failed to rescue from memory deficits.[155] Gantenerumab is another mAb developed targeting the N-terminal and central region of Aβ. The clinical trials gave mixed output with therapeutic benefits and safety concerns.[156] Clinical studies with a larger sample size are underway. Crenezumab is an immunoglobulin G (IgG) mAb that binds to oligomers, fibrils, and plaques to inhibit the Aβ aggregation and dissemble fibrils. The clinical studies revealed that the

mAb is safe at a lower dose and induces microhemorrhages at higher doses.[157] Aducanumab is a potent mAb that targets conformational epitope of Aβ and binds to fibrillar aggregates, which has received conditional FDA approval for AD treatment. The approval was controversial with mixed opinions attributed to its moderate clinical benefits and side effects. Clinical studies demonstrated a beneficial effect with an improvement of cognitive score and change in biomarkers.[158] The therapeutic efficacy and safety profile need to be established by advanced clinical trials.

### 3.3 Metal targeted therapeutics

Metal homeostasis is disturbed in the AD brain with increased metal levels (Cu, Zn, Fe and Al) that strongly bind to Aβ peptide and result in elevated toxicity. These metal ions are known to enhance the aggregation and formation of toxic species. The Aβ-metal ion complex results in oxidative stress and membrane damage, and among them Aβ-copper complexes exacerbate the production of ROS and induce biomolecular damage. The molecules possessing strong metal chelation properties and Aβ interacting ability were explored as AD therapeutics (Fig. 7O).[159] Initially, clioquinol (Clq) was utilised that chelates copper and zinc and exhibit *in vitro* and *in vivo* beneficial effects. Further clinical studies revealed toxic effects and no improvement in the disease condition that results in the failure of the drug.[160] A Clq derivative, PBT2, was developed as a metal-protein attenuator drug candidate for AD. PBT2 inhibits Aβ-metal interaction and reduces Aβ deposition and improves the cognitive performance in a Tg AD mice model.[161] The clinical trial results were ambiguous with safety issues and insignificant therapeutic benefits reported. EGCG is a polyphenolic compound with Aβ aggregation inhibition, antioxidant and anti-inflammatory properties. The EGCG was also found to interact with metal-Aβ species and form unstructured aggregates and reduce toxicity.[162] DP-109 is a lipophilic metal chelator that strongly binds to metal ions and reduces the Aβ burden in the Tg mouse model.[163] The treatment with DP-109 has reduced insoluble Aβ aggregates and supports that the Aβ aggregation is driven by metal ions. Lim and co-workers have developed small molecules based on Clq and stilbene that target metals and Aβ, respectively.[164] The molecules were designed by introducing nitrogen and/or oxygen donor atoms into Aβ interacting molecules to generate effective bifunctional molecules. Molecules 1 and 2 were potent copper chelators, inhibit Aβ aggregation and ameliorate Cu-Aβ mediated neuronal toxicity. A series of compounds were designed based on a selegiline core to target MAO and metal chelation.[165] Among them, compound **8a** displays good MAO inhibition, antioxidant activity, and chelation of biometals (Cu, Zn and Fe). Peptidomimetic P6 developed with GHK tripeptide has displayed good Cu chelation and Aβ aggregation inhibition.[144] P6 sequesters Cu from Aβ peptide and maintains it in a redox dormant state to prevent ROS generation providing an antioxidant effect and protecting biomolecules from oxidative damage. A novel concept of the multipronged drug design strategy was introduced, wherein structural and functional components of known or failed drugs and natural products were integrated to develop hybrid multifunctional modulators (HMMs) to tackle the multifaceted toxicity of AD. TGR86 integrated with structural and functional components of Clq (modulate metal and Aβ toxicity) and EGCG (antioxidant and Aβ modulation) was found to reduce Cu dependent Aβ aggregation and ROS generation by preventing the redox cycle.[140] The molecule successfully inhibits biomolecule and mitochondrial damage and effectively modulates multifaceted Aβ toxicity. We have modified berberine, an isoquinoline natural product, to multifunctional Ber-D, which binds to Cu and forms a ternary complex to prevent ROS generation and exerts antioxidant properties (Fig. 7O).[166] Ber-D inhibits amyloid toxicity and rescues neuronal cells from apoptotic cell death.

### 3.4 Tau targeted therapies

**Targeting post translational modifications (PTMs).** Many kinases that act on tau with glycogen synthase kinase 3 beta (GSK3β) responsible for many tau pathological phosphorylation have been extensively studied.[9,167] Small molecule inhibitors of GSK3β activity were developed and tested for their therapeutic effect to prevent tau pathology (Fig. 8A). Tideglusib is one of the potent GSK3β inhibitors developed and assessed for its clinical use.[168] It was safe in the treatment of AD without any side effects, albeit with no therapeutic benefits. AZD0530 is a potent Fyn kinase inhibitor that was repurposed for AD

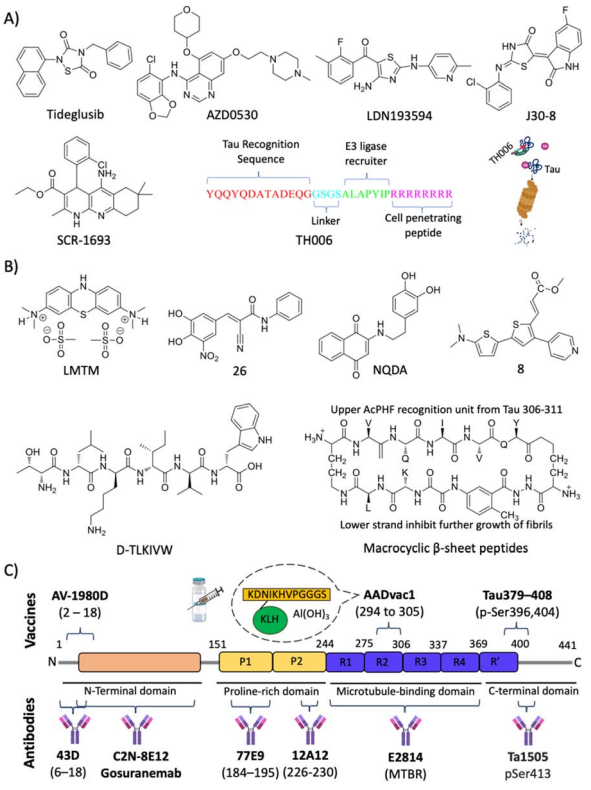


Fig. 8 Tau targeted therapies for AD. (A) Small molecules and peptides targeting post translation modifications. (B) Small molecules and peptide-based molecules for tau aggregation inhibition. (C) Tau targeted active and passive immunotherapeutics.

treatment. An initial clinical trial in AD subjects showed the safety and tolerability of the drug.[169] Studies to assess the therapeutic outcome showed mixed output with no significant disease modification efficacy. Molecules targeting multiple kinases that have implication in tau hyperphosphorylation are projected to be a rational strategy to prevent hyperphosphorylation. The screening series of diaminothiazoles identified LDN193594, which inhibits CDK5 and GSK3β activity with nanomolar $IC_{50}$ (Fig. 8A).[170] The *in vivo* evaluation in the Tg mouse model revealed that LDN193594 is nontoxic, reduces hyperphosphorylated tau tangles, and improves cognitive performance. Recently, a multistage screening approach was adopted to develop an isoform selective inhibitor of JNK3 kinase that has implications for AD.[171] Among the series of 3-substituted indolin-2-one derivatives, J30-8 was found to be a good inhibitor with nanomolar $IC_{50}$ (40 nM) and 2500-fold selectivity towards the JNK3 isoform. J30-8 exhibits *in vivo* biocompatibility, inhibits APP and tau phosphorylation, and improves cognitive performance in the Tg mouse model. A tacrine-based novel molecule SCR1693 was designed and found to promote the dephosphorylation of tau and reduce Aβ production.[172] A chimeric peptide TH006 was designed with three peptide segments with sequences to recognise tau, the second for E3 ligase and the third segment for cell penetration.[173] A tau recognising peptide YQQYQDATADEQG was derived from the β-tubulin sequence (422–434 residues) known to bind tau. The E3 ligase targeting peptide ALAPYIP was derived from von Hippel–Lindau tumour suppressor protein (VHL), a substrate for E3 ligase. The designed peptide targets tau protein for ubiquitin degradation, and reduces tau levels in primary neurons and the Tg AD mouse model (Fig. 8A).

**Microtubule stabilisers.** It is perceived that hyperphosphorylated tau detaches from the microtubule and destabilises, leading to pathological consequences in neurons. Keeping this fact in mind, drugs that were used in cancer as microtubule stabilisers have been repurposed for AD.[19] Epothilone D, a brain permeable microtubule stabiliser, was assessed for therapeutic effects in an old age tau mouse model.[174] There was a significant improvement in microtubule density that restores axonal transport and cognitive performance with a reduction of tau burden in the forebrain and enhanced neuronal integrity. A microtubule stabiliser abeotaxane (TPI-287) was evaluated for repurposing and the drug treatment resulted in severe hypersensitive reactions in AD cases and worsening of conditions in other tauopathies.[175]

**Tau aggregation inhibition.** Molecules that inhibit the tau aggregation process halt the formation of toxic species and rescue neuronal cells. Many small molecules that effectively inhibit tau aggregation have been explored (Fig. 8B).[176] Methylene blue (MB) is BBB permeable and demonstrated to reduce tau aggregation. Leuco-methylthioninium bis(hydromethanesulphonate) (LMTM), a modified MB, was effective in preclinical studies. Initial clinical studies demonstrated safety and good pharmacokinetics, which did not translate into significant disease modification.[177] However, prolonged LMTM monotherapy in a large clinical study showed improvement in brain atrophy and cognitive performance. Nitrocatechols were screened for tau aggregation modulation and found that compound **26** exhibits good anti-aggregation activity.[178] Detailed *in silico* studies to understand the mode of interaction of compound **26** with the VQIVYK steric zipper revealed that **26** is oriented parallel to the fibre axis. The nitrocatechol moiety of **26** is engaged in polar interactions with Gln and Lys side chains and the aromatic ring makes van der Waals come in contact with the Val side chain. The cyano group in the molecule forms two hydrogen bonds with $NH_3^+$ of two Lys side chains and amide carbonyl was engaged in hydrogen bonding with Lys residue. An unsubstituted benzyl ring is involved in π-cation interaction with $NH_3^+$ of Lys residue. All these attributes have contributed to the strong interaction of **26** with tau and subsequent inhibition of its aggregation. A naphthoquinone-dopamine hybrid molecule NQ-DA was designed to target tau aggregation.[179] The molecule targets PHF (VQIVYK) and PHF* (VQIINK) motifs and effectively inhibits the tau aggregation. We have screened a focussed library of thiophene-based small molecules and identified compound **8** with anti-aggregation activity and rescued SH-SY5Y cells from tau toxicity.[180]

Eisenberg and co-workers have designed structure-based peptides of unnatural amino acids and identified an all D-peptide (D-TLKIVW) inhibitor of tau aggregation (Fig. 8B).[181] The peptide targets the steric zipper motif of tau and successfully inhibits seeded and non-seeded tau aggregation. Macrocyclic β-sheet peptides were designed with an upper strand of a pentapeptide with two delta linkers of the ornithine moiety and a lower strand composed of 2 residues and a β sheet peptidomimetic Hao template (Fig. 8B).[182] The designed peptidomimetics adopt β-sheet conformation and effectively inhibit the aggregation of PHF motif peptides. Structure-based short peptides from the VQIINK aggregation driver were designed and these peptides effectively inhibit the aggregation of full-length tau protein and the seeding effect of exogenous tau fibrils.[183] We have reported peptoids derived from the KLVVF motif of Aβ and their effect on tau aggregation along with controls LPFFD and KLVFF.[184] Hybrid peptoids P4 and P5 retained the tau in its random coil state as revealed by CD spectroscopy, inhibiting tau aggregation and rescuing neruro2a cells from tau toxicity.

**Immunotherapy.** Many vaccine candidates were developed from pathogenic fragments, and phosphorylated epitopes of tau and mAbs targeting different regions of tau were evolved with potential therapeutic benefits under clinical trials (Fig. 8C). DC8E8 mAb revealed an epitope spanning 294 to 305 amino acid residues, which was essential for pathogenic tau–tau interaction. A peptide vaccine AADvac1 was derived from this region (KDNIKHVPGGGS) and tested in a Tg rat model.[185] In a phase 2 clinical trial, the vaccine was given for a longer duration with repeated doses and it was found that the vaccine was safe.[186] There was increased IgG titre indicating good immunogenicity but no improvement in cognitive performance. Prophylactic immunisation of the Tg mouse demonstrated the efficacy of the tau379–408[P-Ser396,404] vaccine.[187] The prophylaxis elicited antibody response and reduced both tau and Aβ burden and microgliosis. A DNA based vaccine AV-1980D targeting the N-terminus of tau was constructed using the Mutli-TEP platform.[188] The vaccine triggers a good humoral

immune response against tau and ameliorates tau pathology in a THY-tau22 mouse model. This demonstrated the possible applications of DNA and RNA-based immunotherapeutics for AD.

A humanised anti-tau antibody C2N-8E12 (ABBV-8E12) was developed, which reduces tau burden and rescues cognitive impairments.[189] Phase 1 clinical investigation revealed the safety, good pharmacokinetics, and brain uptake with poor immunogenicity. BIIB092 (Gosuranemab, BMS-986168) is a mAb selectively targeting the N-terminal fragment of tau.[190] Preclinical studies are promising, and the clinical safety studies showed tolerability up to 2100 mg dose. The treatment of a Tg mouse model with mAb Ta1505 developed against pSer413 has reduced tau burden and improved synaptic density and cognitive deficits.[191] Preclinical evaluation of two mAbs 43D (against tau 6–18) and $77 \times 10^9$ (against tau 184–195) revealed a reduction of tau burden and rescued from cognitive deficits.[192] Six doses of 43D mAb effectively reduced total tau, hyperphosphorylated tau and rescued the 3xTg mouse model from spatial and short-term memory. Interestingly, a reduction in Aβ peptides and aggregates in the hippocampus was observed, which iterates the therapeutic potential of 43D mAb. Recently, 12A12 mAb that selectively binds to a pathologically relevant neurotoxic NH226-230 fragment has been explored for its beneficial effect in two different Tg mouse models.[193] The treatment has neutralised the target tau, reduced tau and Aβ burden, and improved learning and memory deficits. The antibody reduced gliosis and rescued dendritic spine connectivity and hippocampal long-term potentiation (LTP). A high affinity mAb E2814 that binds to the microtubule binding region (MTBR) was developed ($K_d$ = 88 pM).[194] The results are promising in the Tg mouse model with mAb reducing the seeding, transmission, and tau burden. Many passive immunisations using novel mAb are in clinical trials and show promising results in early clinical studies. The success of mAb therapy in phase 3/4 clinical trials is yet to be disclosed.

### 3.5 Targeting ROS and oxidative stress

Elevated levels of ROS and oxidative stress in the AD brain compelled researchers to consider antioxidant molecules as therapeutic candidates to combat the disease pathology (Fig. 9A). There is an inter-relation between Aβ-metal ions in the production of ROS and oxidative stress.[4,8,159,195] Aβ peptide has metal binding sites and the redox metal ions bound to the peptide generate excess ROS. Copper is a strong redox metal ion that in complexation with Aβ results in excess ROS generation causing membrane (lipid), DNA, and protein damage. These events elevate the oxidative stress of neuronal cells which leads to neurodegeneration. Vitamin E and selenium are natural bioavailable antioxidants and show beneficial effects in *in vitro*

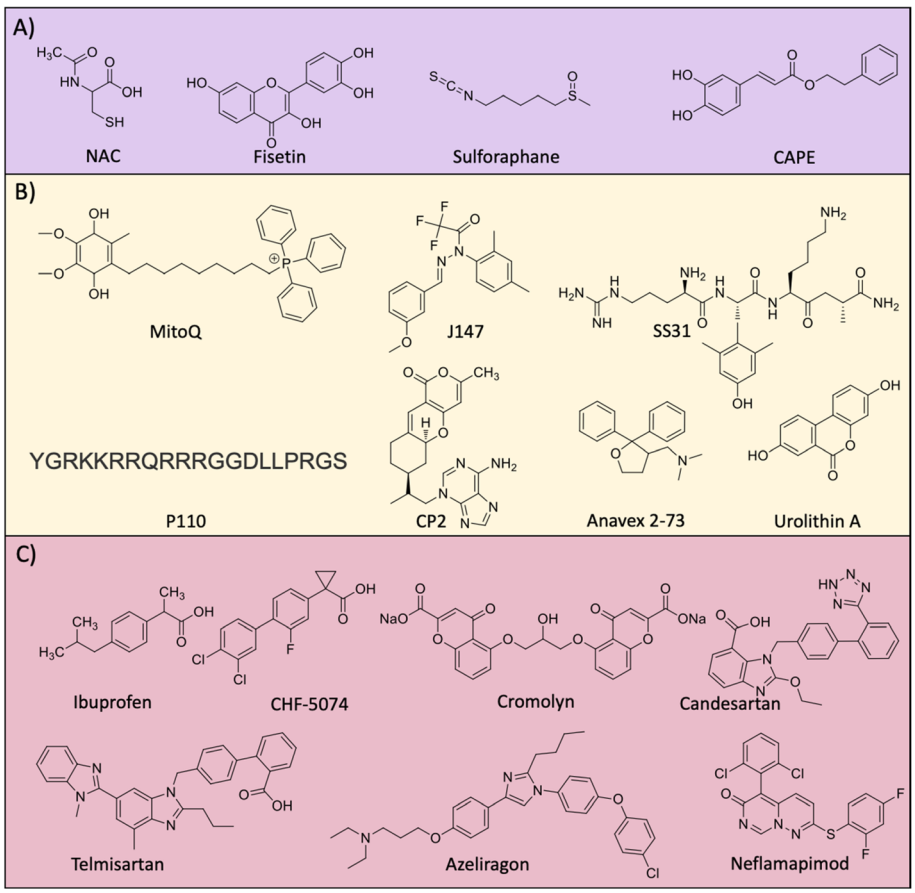


Fig. 9 Molecules targeting (A) oxidative stress, (B) mitochondrial damage and (C) neuroinflammation.

and *in vivo* studies. Dietary supplementation individually and in combination to AD patients has minimal beneficial effects and the overall results are ambiguous.[196] Glutathione (GSH) is a natural tripeptide (γ-L-glutamyl-L-cysteinyl-glycine) produced in the body that has antioxidant activity. GSH acts as a cytoprotective molecule by effectively scavenging ROS, thereby reducing biomolecular damage and oxidative stress. The brain GSH level is reduced in the case of AD causing pronounced oxidative stress, and hence therapeutics elevating GSH levels is a rational approach to treat AD. *N*-Acetyl-L-cysteine (NAC) treatment is known to elevate the levels of GSH and imparts an antioxidant effect. The treatment of aging rat models with NAC increases the antioxidant enzymes and molecules.[197] Recently, a study uncovered that patients with flavanol intake as part of their diet had a reduced risk of AD.[198] These results suggest the possible therapeutic potential of flavonols and further need to explore the effect of dietary flavanols for AD treatment. Resveratrol is a natural antioxidant utilised as an AD therapeutic with beneficial effects.[199] The beneficial effect of resveratrol was shown in many *in vitro* and preclinical study and clinical trial results revealed mixed output. Fisetin was assessed for its antioxidant and anti-inflammatory effect in an aging rat model.[200] The alleviation of the oxidative stress and neuroprotective effect of the compound underscore fisetin as a potential anti-AD drug candidate. Nuclear factor-erythroid factor 2-related factor 2 (Nrf2) is a transcription factor that is activated to induce the expression of many antioxidant genes to counteract oxidative damage. Sulforaphane was reported to upregulate Nrf2 expression by decreasing methylation in the promoter region and rescue neuronal cells (Fig. 9A).[201] The compound reduced Aβ levels and inflammatory mediators and increased cellular antioxidants in a cell model. Caffeic acid phenethyl ester (CAPE) is a potent antioxidant and anti-inflammatory agent assessed for its activity against Aβ oligomers and induced toxicity in the Tg mouse model.[202] Treatment induces the expression of Nrf2 and counteracts oxidative stress, apoptosis, neuroinflammation, and rescue memory and cognitive deficits. We have developed GHK-based small molecules that target Aβ and metals, and reduce ROS to rescue from oxidative stress as evident from the emulation of Nrf2 action.[203]

### 3.6 Mitochondrial dysfunction

The accumulation of Aβ and tau aggregates, ROS and oxidative stress results in mitochondrial damage and many therapeutics have been developed targeting mitochondria (Fig. 9B). MitoQ was developed by integrating a mitochondria targeting moiety ($PPh_3$) with a hydroquinone moiety as a potent antioxidant to reduce the mitochondrial damage.[204] The treatment with MitoQ in a Tg AD mouse model for a longer period was safe, reduced Aβ load, oxidative stress, and neuroinflammation and alleviated cognitive decline. The design strategy of integrating a mitochondria targeting moiety with diagnostic and therapeutic molecules has potential for AD diagnostics and therapeutics.[204,205] J147 is a curcumin analogue targeting mitochondria to improve memory and cognitive deficits in a Tg AD mouse model.[206] Mechanistic study reveals that J147 targets ATP synthase in mitochondria and increases the intracellular calcium that leads to the activation of the AMPK/mTOR pathway for improvement in longevity. In AD, multiple pathological factors trigger mitochondrial damage and result in the alteration of mitochondrial dynamics with decreased fusion, increased fission and biogenesis.[207] The mitochondrial fission is mediated by Drp1 and Fis1 proteins that interact to fragment the damaged mitochondria. The beneficial effects of tetrapeptide SS31 were assessed in a Tg AD mouse model and it was found that it crosses BBB, inhibits mitochondrial fission, reduces soluble Aβ and enhances synaptic function.[208] Resveratrol was shown to act on mitochondrial fission and biogenesis to maintain mitochondrial homeostasis.[209] The compound also positively influences energy metabolism with glucose utilisation and ATP production. The rationally designed peptide-based inhibitor of mitochondrial fission P110 inhibits Drp1/Fis1 interaction.[210] P110 treatment in Tg AD effectively reduced mitochondrial fission and Aβ accumulation, and rescued from energy imbalance and oxidative stress that underscores the possible clinical implications. Targeting complex **1** of mitochondria to suppress its activity was achieved by small molecule CP2.[211] It was evident that treatment with CP2 reduced Aβ and tau burden in the Tg mouse model. CP2 also reduces the activity of GSK3β and restores axonal transport with multiple beneficial effects. The sigma 1 receptor (S1R) is expressed in the endoplasmic reticulum and its function is altered in AD.[212] It is a ligand operated receptor that mediates protein homeostasis, synaptic plasticity, and neuroprotection. Anavex 2–73 is a small molecule agonist for S1R that is known to induce the misfolding protein rescue response.[213] The compound was safe and improve cognition in a dose dependent manner in mild to moderate AD cases. The abnormal mitophagy is evident in the hippocampus of the human AD brain and induction of mitophagy by urolithin A reduces Aβ and tau burden and rescues memory and cognitive deficits in the Tg mouse model.[214] The work demonstrated the role of mitophagy and mitophagy inducers as potential therapeutic candidates for AD. TGR86 that reduced ROS production and Aβ aggregation effectively prevents Aβ induced mitochondrial damage.[140] BerD exhibits mitochondrial protection as shown by the rescue of cells from Aβ induced mitochondrial membrane potential (MMP) disruption and Cyt c mediated apoptotic cell death.[166]

### 3.7 Neuroinflammation

Neuroinflammation is a pathological event that occurs in the early stage of AD. Therapeutic developments targeting neuroinflammation using novel drugs and repurposing of available anti-inflammatory drugs have been explored (Fig. 9C).[215] Non-steroid anti-inflammatory drugs (NSAIDs) like ibuprofen, tarenflurbil, and CHF5074 were assessed for their anti-neuroinflammatory properties and encouraging results *in vitro* and *in vivo* preclinical studies were found.[216] Despite having good safety profiles, most of them failed to improve cognition deficits in clinical studies. Combinational therapy of ibuprofen and cromolyn (ALZT-OP1) is under a phase 3 clinical trial (NCT02547818) and results are yet to be disclosed.

Sargramostim is a synthetic granulocyte-macrophage colony-stimulating factor that stimulates the innate immune system to increase activated microglia and reduction in Aβ load, and increased synaptic area and cognitive performance. Clinically, the drug was safe and improve cognitive performance with a better MMSE score.[217] Angiotensin1 receptor (AT1R) activation expressed on microglial cells and astrocytes induces neuroinflammation. Candesartan, a potent AT1R blocker exhibits anti-neuroinflammatory effects in the Tg AD mouse model.[218] The compound shifted microglial activation towards the neuroprotective phenotype, alleviates lipopolysaccharide (LPS) treated neuroinflammation and significantly reduces the Aβ burden in a Tg AD mouse model. Telmisartan is another AT1R blocker developed as intranasal administration for the amelioration of neuroinflammation.[219] Treatment with telmisartan reduces Aβ burden, microglial activation, and neuronal loss and improves the spatial memory of a 5xFAD Tg mouse leading to evaluation in clinical trials. GC021109 is a novel compound reported to target directly microglial cells on the purinergic P2Y6 receptor. The treatment modulates microglial cells to clear Aβ aggregates and reduced the release of proinflammatory mediators and a clinical study to assess the safety and efficacy was undertaken and the results are yet to be disclosed (NCT02386306).[220] Receptors for advanced glycation end products (RAGE) are expressed on glial cells and RAGE activation was shown to play a role in AD pathology.[221,222] Azeliragon is an orally active small molecule developed as a RAGE inhibitor, which showed to reduce Aβ burden, neuroinflammatory mediators and cognitive performance.[223] The drug was effective in mild AD cases and is currently under a phase 3 clinical trial. Tumor necrosis factor alpha (TNFα) is one of the major mediators of neuroinflammation and downstream of the TNFα signalling pathway, p38a regulates the pathway. Neflamapimod is a small molecule inhibitor of p38a that improves synaptic dysfunction and reverses memory deficits. Clinical evaluation in mild to moderate AD cases showed that the drug is safe and well tolerated, but there was no improvement in episodic memory.[224] Significant alteration was observed for CSF t-tau, p-tau and neurogranin, which indicates that the higher dose and longer duration of treatment possibly benefit the AD patients. We recently reported a multifunctional small molecule M3 that effectively reduced microglial activation and neuroinflammation.[225] M3 effectively inhibits NF-κβ mediated neuroinflammation and reduces TNFα levels in Aβ activated microglial cells.

### 3.8 Multifunctional modulators – future of AD drug discovery

Drugs developed against different individual targets encountered failure and some are in clinical trials. Aβ targeted drug discovery over the last two decades encountered limited success and search for novel tangible targets is necessary. In addition to Aβ, tau is considered a potential target and many therapeutic candidates are developed. Among them, immunotherapeutics are on the road to success in early clinical studies. Many other

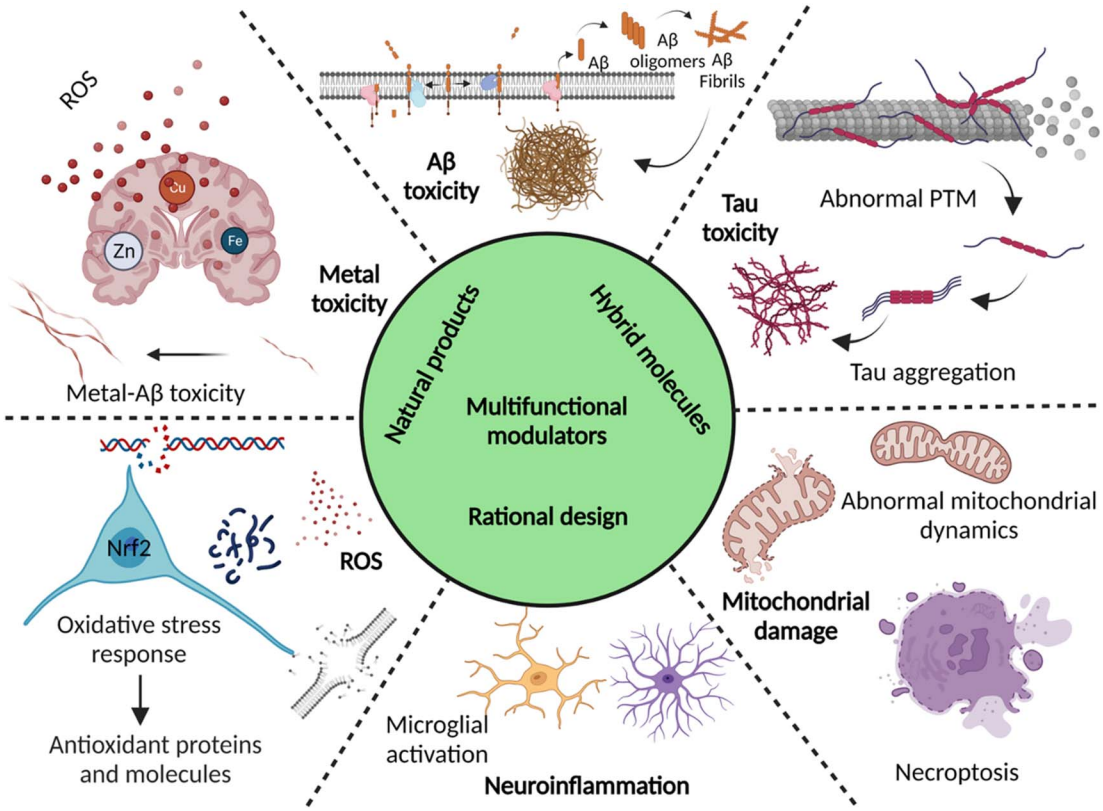


Fig. 10 Multifunctional modulators targeting multiple disease pathological pathways of AD (created with BioRender.com).

targets that were considered in the last decade are discussed *vide supra*. The multifactorial nature of AD and failures in drugs targeting a single pathological target emphasise the need for multifunctional therapeutics to tackle multiple disease causative factors. Recent understandings of various aetiological factors associated with AD helps to design chemical tools to target multiple disease pathologies.[226] Natural products have been tuned to develop multifunctional molecules to target metal dependent and independent Aβ toxicity.[227] Molecular architecture has been fine tuned to generate Aβ, metal and ROS targeting small molecules.[228] Few combination therapies and dual targeting molecules were developed with better therapeutic benefits. We propose multifunctional small molecules that target multiple disease targets as potential future drug candidates for AD (Fig. 10).[4,8,9,17] These molecules are anticipated to synergistically alleviate complex AD pathology and future therapeutics for AD.

**Aβ and tau dual aggregation modulators.** A curcumin derivative PE859 was developed to target both Aβ and tau aggregation effectively reduced Aβ and tau load and improved cognitive deficits in a mouse model (Fig. 11).[229] 1,2,3,4-Tetrahydro-1-acridone derivative 30 is reported as a dual inhibitor of Aβ and tau and reduces Aβ and tau aggregation and associated toxicity in a cellular milieu with good brain uptake.[230] Hybrid peptoids P4 and P5 modulate both Aβ and tau aggregation.[143,184] These peptoids effectively rescue neuronal cells from Aβ and tau toxicity. Recently, we have screened a focused library of 52 thiophene-based small molecules targeting Aβ aggregation and identified five lead candidates.[180] The detailed ThT assay, dot blot assay, gel electrophoresis and transmission electron microscopy (TEM) results demonstrated compound **8** as a good modulator of Aβ and tau aggregation. Compound **8** is non-toxic up to 100 μM and rescues neuronal cells from both Aβ and tau toxicity.

**Hybrid multifunctional inhibitors targeting multiple targets.** Shogaol–huprine hybrid molecules were synthesised and screened *in vitro* for their multifunctional activity (Fig. 11).[231] The compounds show good inhibition of AChE and BACE1 enzymes with Aβ and tau aggregation inhibition activity. A series of *N*-benzylpiperidine derivatives were synthesised, and among them 41 was found a potent inhibitor of AChE and BACE1 enzymes, antioxidant, and Aβ aggregation inhibitor, and crosses BBB and alleviates scopolamine induced cognitive deficits (Fig. 11).[232] Tetrahydroisoquinoline-benzimidazole hybrid molecules were synthesised as multifunctional agents and screened for the inhibition of BACE1 and neuroinflammation by the reduction of nitric oxide (NO) production.[233] Among all, BD3 exhibits good anti-inflammatory activity with moderate BACE1 inhibition and neuroprotective effects by combating ROS in neuronal cells (Fig. 11). The conjugate of

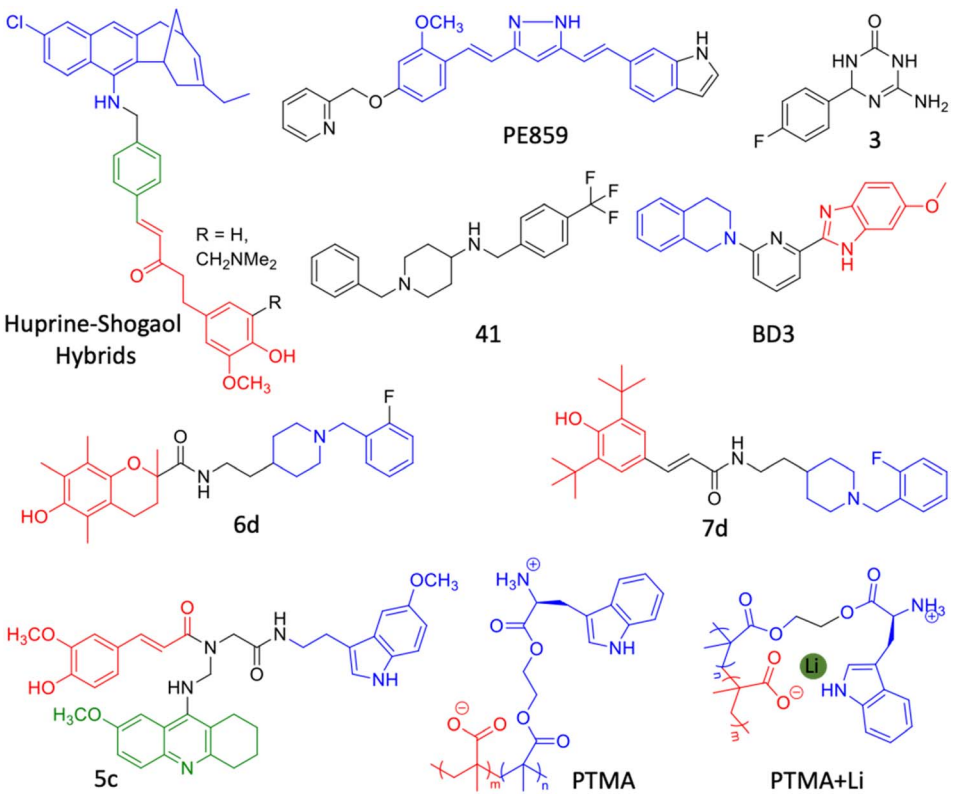


Fig. 11 Hybrid multifunctional modulators targeting multiple therapeutic targets of AD (blue: huprine moiety, red: shogaol moiety and green: conjugated benzene ring for Aβ and tau aggregation inhibition in the huprine–shogaol hybrid; blue: curcumin moiety in PE859; blue: tetrahydroisoquinoline moiety and red: benzimidazole moiety in BD3; blue: donepezil moiety and red: trolox moiety in **6d**; blue: donepezil moiety and red: butylated hydroxytoluene moiety in **7d**; blue: melatonin moiety, red: feruloyl moiety and green: tacrine moiety in **5c**; blue: tryptophan based polymer and red: polymethyl acrylate in PTMA).

trolox, an antioxidant, and donepezil, an AChE inhibitor, (**6d**) displays optimal activity against AChE, MAO and a potent antioxidant (Fig. 11).[234] Compound **6d** inhibits metal independent and copper dependent Aβ aggregation and rescue memory deficits in a scopolamine induced mouse model. Donepezil and a potent antioxidant butylated hydroxytoluene (BHT) were conjugated to develop hybrid molecules, of which **7d** displayed balanced activity towards AChE and MOA inhibition, antioxidation, and anti-aggregation of Aβ peptide (Fig. 11).[235] **7d** reduced LPS induced neuroinflammation, crossed BBB and reduced cognitive deficits in the scopolamine induced mouse model. Multifunctional tacrines were developed by integrating with ferulic acid and melatonin to reduce oxidative stress.[236] Compound **5c** exhibits potent antioxidant activity and AChE inhibition, and inhibits oxidative stress through Nrf2 induction and the neuroprotective effect.

The development of dual inhibitor targeting of BACE1 and GSK3β responsible for Aβ and tau accumulation is a tangible approach. In this direction, triazinone derivative **3** is reported as an effective dual enzymes inhibitor (Fig. 11).[237] Compound **3** showed a neuroprotective effect in cellular models and crossed BBB in the mouse. Hybrid conjugate **6** of tacrine and valmerin linked through a triazole linker inhibits AChE and GSK3β activity with nanomolar $IC_{50}$, is nontoxic to neuronal cells and crosses BBB (Fig. 11).[238] We have designed a diblock copolymer-based polyampholyte (PTMA) with tryptophan to impart biocompatibility, lithium (Li) encapsulation and intrinsic fluorescence to monitor the binding and Li release (Fig. 11).[239] The designed PTMA effectively inhibits Aβ aggregation and dissolves the preformed fibrillar aggregates. PTMA is biocompatible with minimal toxicity up to 100 μM and rescues neuronal cells from Aβ toxicity. PTMA effectively encapsulates Li, delivers to cells and releases at acidic pH (endosome) in a stimuli responsive and controlled manner, which can be monitored by intrinsic fluorescence off-on modulation. Li therapy is considered viable to treat AD through possible inhibition of GSK3β by electrostatic and cation–π interactions. The Aβ aggregation modulation and effective Li delivery of PTMA underscore its potential for combinational therapy for AD and other neurological disorders.

**Rationally designed multifunctional modulators targeting multitargets.** Many therapeutic molecules were rationally designed to target different pathological aspects of AD. The structural and functional information deduced from the previous drug molecules was employed to design potent multifunctional modulators (MFMs) by hybridisation, functionalisation and conjugation of active components of synthetic or natural origin and integration of multiple active subunits (Fig. 12). We have designed a multifunctional peptidomimetic modulator P6 by conjugation of GHK tripeptide (a natural Cu chelator) with Aβ aggregation modulating hybrid peptoid.[144] P6 inhibits the aggregation of Aβ to form oligomers, fibrils, and oligomer mediated membrane damage. P6 strongly chelates Cu, inhibits Cu dependent Aβ aggregation, and sequesters Cu from the Aβ-Cu inclusion complex to reduce ROS generation and DNA damage. The sarcosine incorporation in the peptide sequence imparts serum stability to P6, biocompatible and rescue neuronal cells from Aβ toxicity. Lee *et al.* rationally designed small molecule ML by integrating structural components to inhibit Aβ aggregation, metal chelation and antioxidant activity (Fig. 12).[240] ML reduced Aβ and Aβ-metal toxicity and ROS and is BBB permeable. Another small molecule DMPD was designed by tuning redox properties to redirect Aβ peptide to nontoxic off pathway aggregate formation through covalent adduct formation (Fig. 12).[241] Detailed biochemical, biophysical, and MD simulation studies have showed that ligand-peptide adduct formation was through primary amine-dependent intramolecular cross-linking. DMPD treatment in a 5xFAD Tg mouse model has significantly reduced Aβ load and rescued from memory deficits. HMMs were developed by integrating 8-hydroxy quinolone moieties from Clq (as a metal chelator) and Aβ inhibition with a polyphenolic moiety from EGCG for antioxidant properties in a single molecule.[140] Among them, TGR86 exhibits better Aβ aggregation inhibition by hydrogen bonding, alkyl interaction and interruption of the salt bridge (Lys28-Asp23). TGR86 effectively chelates Cu and reduces Cu-dependent Aβ aggregation and ROS generation *in vitro* and in cellulo. HMM effectively reduces ROS-associated DNA and protein damage. The designed HMM was non-toxic compared to Clq and rescue neuronal cells from multifaceted Aβ toxicity. The multifunctional effect of TGR86 effectively prevented mitochondrial damage as demonstrated by the rescue of Aβ induced MMP disruption. A series of molecules were designed by conjugating amino acids, L-dopa and dopamine with a naphthalene diimide (NDI) core to develop multifunctional modulators (Fig. 12).[242] Among them, L-dopa and dopamine derivatives NLP and NDP, respectively, inhibit Aβ aggregation and dissolve preformed fibrils. *In silico* docking studies showed that compounds bind to aggregation driving KLVFFA and IIGLM motifs. NLD and NDP exhibit good antioxidant activity and rescue neuronal cells from Aβ toxicity.

Han *et al.* fine-tuned an *N*,*N*-dimethylaniline (DMA) moiety to develop bidentate ligands of different oxidation potential, with antioxidant and metal chelation properties.[243] DMA1 with the lowest oxidation potential ($E_{pa}$ = 0.22 V) displays noticeable modulation of metal dependent and independent Aβ aggregation with radical scavenging activity (Fig. 12). DMA2 with moderate oxidation potential ($E_{pa}$ = 0.54/0.80 V) exhibits significant inhibition of Cu(II)-Aβ aggregation, whereas DMA3 with higher oxidation potential ($E_{pa}$ = 0.75 V) shows a poor

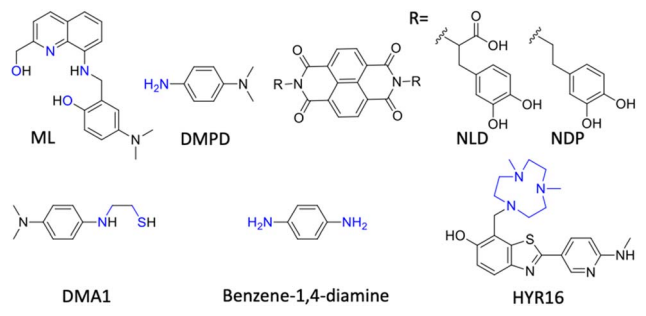


Fig. 12 Multifunctional modulators (MFMs) targeting multiple pathological facets of AD (blue: metal chelating moiety in structures).

modulatory effect. They further explored the phenylene moiety to design simple molecules with a minimalistic approach based on redox principles to target multiple disease targets.[244] Benzene-1,4-diamine exhibits reactivity with free radicals and Aβ in free as well as metal bound states to retard aggregation (Fig. 12). Mechanistic studies revealed that the redox properties of the molecule favour the chemical modification of Aβ peptide by the formation of a chemical adduct that inhibits Aβ aggregation. *In vivo* treatment with compound results in reduced Aβ load and rescues from memory and cognitive deficits in a Tg AD mouse model. Mirica and the group developed MFMs with therapeutic benefits and imaging abilities (Fig. 12).[38] MFMs were designed by combining benzothiazole, an Aβ binding moiety, with a strong Cu chelating 1,4-dimethyl-1,4,7-triazacyclononane (tacn) group. Among the MFMs, HYR-16 showed the prevention of Cu-mediated toxic oligomer formation, metal chelation and ROS scavenging. Ber-D with polyphenolic groups imparts better Cu chelation and antioxidant properties and reduces toxicity by reducing the interaction of Aβ aggregation species with a mitochondrial membrane.[166] Ber-D effectively reduces metal independent and dependent Aβ aggregation. MD studies revealed the formation of a BerD-Aβ-Cu tetrahedral cooperative complex that ameliorates Cu-Aβ toxicity. The interaction analysis of Aβ42 monomer and Ber-D revealed that the Aβ42:Ber-D complex is stabilised by hydrogen bonding with His6 and His14 residues and two hydrogen bonds with Asp7 residue. *In vitro* studies showed antioxidant activity, reduced ROS and oxidative stress, and inhibited DNA and protein damage. Ber-D rescues PC12 neuronal cells from Aβ toxicity and apoptotic cell death. This natural product-derived molecular platform can be explored to develop MFMs for multifaceted AD pathology.

**Multifunctional modulators targeting amyloid toxicity, mitochondrial damage and neuroinflammation.** GHK exhibits high affinity for Cu and modulates Cu-dependent multifaceted Aβ toxicity. To impart true multifactional properties, we

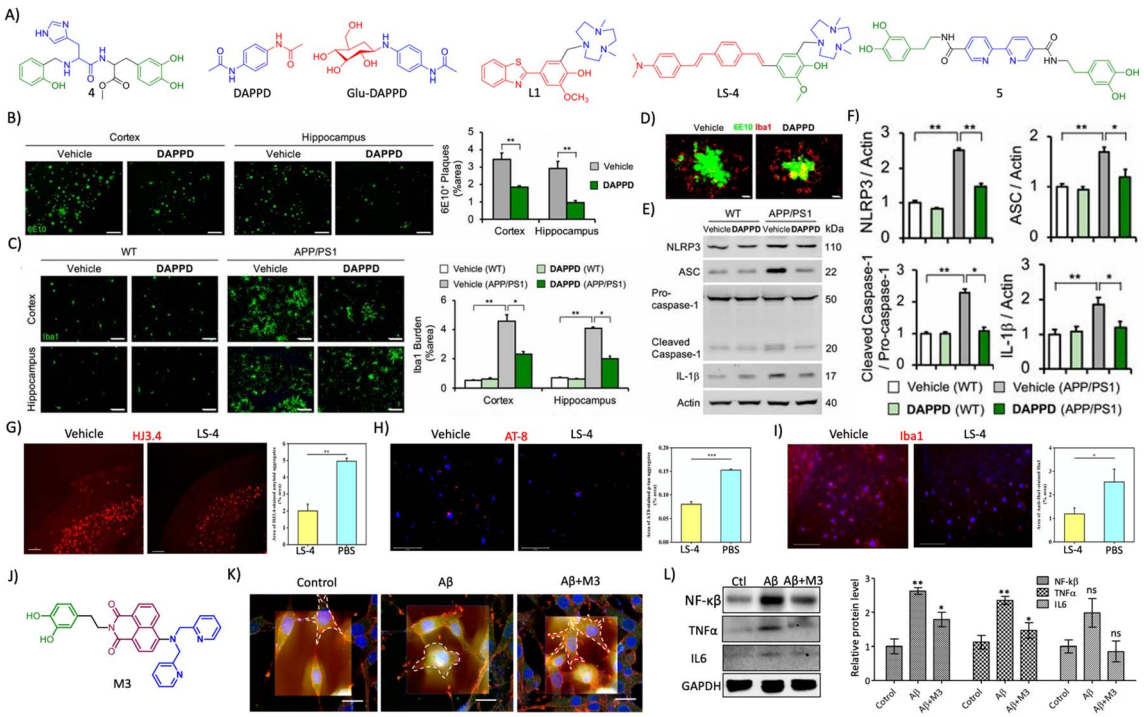


Fig. 13 (A) Rationally designed multifunctional modulators targeting amyloid associated toxicity and neuroinflammation (blue: metal targeting moiety and green: L-dopa for antioxidant and anti-inflammatory activity in **4**; blue: phenylacetamide moiety for neuroprotection and red: acetamide moiety for lipophilicity and stability in DAPPD; blue: DAPPD moiety and red: glucose moiety for BBB crossing in Glu-DAPPD; blue: triazacyclononane metal chelating moiety and red: 2-phenylbenzothiazole based Aβ targeting moiety in L1; blue: triazacyclononane metal chelating moiety, red: distyrylbenzene Aβ targeting moiety and green: vanillin based antioxidant moiety in LS-4; blue: 2,2′-bipyridine moiety for metal chelation and green: dopamine for antioxidant activity in **5**). (B) Reduction of amyloid plaques (6E10 staining, scale bar 200 μm) and (C) microglial activation (Iba1, scale bar 50 μm) by DAPPD treatment in WT and APP/PSEN1 Tg mice. (D) Colocalisation of Aβ plaques with microglial cells in DAPPD treated cells (scale bar 10 μm). (E) Western blot analysis of NLRP3 and associated neuroinflammatory proteins and (F) its quantification in DAPPD treated WT and APP/PSEN1 mice brain samples. (B)– (F) Reproduced from ref. 245 with permission from PNAS, copyright 2019. (G) Immunofluorescence images of brain sections of 5xFAD mice treated with LS-4 stained for Aβ and quantification shows the reduction in Aβ load (scale bar 500 μm). (H) Reduction of tau aggregates by treatment with LS-4 as shown by AT8 staining and quantification (scale bar 125 μm). (I) LS-4 treatment ameliorates microglial activation as revealed by Iba1 immunofluorescence and its quantification (scale bar 125 μm). (G)–(I) Reproduced from ref. 248 with permission from the American Chemical Society, copyright 2021. (J) Structure of multifunctional modulator M3 (blue: DPA moiety for metal chelation, red: NMI for Aβ targeting and green: dopamine for antioxidant and anti-inflammatory activity). (K) Bio-AFM characterization of microglial activation and its reduction by M3 (scale bar 20 μm). (L) Western blot analysis of NF-κβ, TNFα and IL6 and its quantification in M3 treatment for its anti-neuroinflammatory effect. (K) and (L) Reproduced from ref. 225 with permission from the American Chemical Society, copyright 2022.

modified the structure to obtain a set of MFMs (Fig. 13A).[203] Among them, MFM 4 effectively chelates Cu and Fe and silences the redox cycle to inhibit ROS generation *in vitro* and in cellulo. The antioxidant moiety L-dopa aid effectively quenches ROS, reduces oxidative stress and DNA damage and modulates Nrf2 signalling. MFM 4 inhibits Aβ aggregation and rescues neuronal cells from Aβ toxicity. NMR study showed the ability of MFM 4 to interact with Aβ42 by specific hydrogen bonding and aromatic interactions. It reduces mitochondrial damage as measured by MMP and NO production in LPS induced microglial cells. A small molecule *N*,*N*′-diacetyl-*p*-phenylenediamine (DAPPD) is reported, which is capable of promoting the phagocytic activity of microglial cells (Fig. 13A).[245] DAPPD consists of a phenylacetamide moiety that is structurally similar to acetaminophen, a known anti-neuroinflammatory drug, and an acetamide moiety that imparts lipophilicity and metabolic stability. Hence DAPPD is expected to be a good anti-neuroinflammatory compound with BBB permeability and bioavailability. The study has demonstrated that DAPPD effectively promotes microglial phagocytosis, clears Aβ load and reduces NLRP3 associated proinflammatory mediators through NF-κβ suppression in a Tg mouse model (Fig. 13B–F). The compound treatment effectively rescues memory and cognitive impairments. To overcome the limitations, the prodrug Glu-DAPPD has been designed by conjugating with the glucose that increases solubility and enhances brain uptake by GLUT1 receptor mediated transport across BBB (Fig. 13A).[246] Glu-DAPPD was effective in the reduction of Aβ load and neuroinflammation and improving cognitive function. A multifunctional molecule L1 was constructed by integrating a 2-phenylbenzothiazole based Aβ interacting group with a triazacyclononane (TACN) macrocyclic group for metal chelation (Fig. 13A).[247] The designed molecule is a metal chelator and antioxidant and rescues neuronal cells from metal dependent Aβ toxicity. L1 crosses BBB, modulates Aβ and tau burden and reduces neuroinflammation in a 5xFAD Tg mouse model. Similarly, potent theranostic agents were constructed by integrating a distyrylbenzene moiety with metal chelating triazamacrocycle and antioxidant vanillin groups (Fig. 13A).[248] LS-4 emerged as an efficient theranostic agent that reduces Aβ and tau aggregates and microglial activation (Fig. 13G–I). Recently, we have designed and synthesized an array of multifunctional modulators by curating the metal-chelating properties of 2,2′-bipyridine with the functional and structural properties of unique Aβ42 targeting biomolecular auxiliaries.[249] The bipyridyl core functionalised with dopamine (**5**) displayed metal-chelation, excellent modulatory efficiency against metal-independent and -dependent Aβ42 aggregation, ROS/reactive nitrogen species (RNS) generation, oxidative stress and neuroinflammation, thus serving as a promising MFM to ameliorate AD pathology. We developed multifunctional modulators by integrating a NMI core with a metal chelating dipicolylamine moiety and dopamine with an antioxidant, and anti-inflammatory properties.[225] Among the designed modulators, M3 with all three pharmacophore units effectively alleviates multifaceted Aβ toxicity (Fig. 13J). *In vitro* studies demonstrated that M3 modulates metal independent and dependent Aβ aggregation and antioxidant activity and reduces oxidative stress in neuronal cells as evident from the suppression of Nrf2 stress response. M3 synergistically reduces mitochondrial damage as evident from the rescue of structural and functional damage, by inhibiting localisation of Aβ in mitochondria, and reduces Cyt c levels and apoptotic cell death. A detailed nano-mechanical and molecular study by Bio-AFM and western blot analysis revealed the ability of M3 to reduce microglial activation and NF-κβ mediated neuroinflammation (Fig. 13K and L). This work demonstrates the rational design of MFMs to synergistically target multiple AD pathologies for excellent therapeutic benefits. Such rationally designed MFMs have high potential as future AD therapeutics.

## 4. Conclusion and future prospects

High prevalence of the disease and the absence of reliable diagnostics and therapeutics reiterates the need for adopting holistic approaches towards identifying better disease management strategies. The clinically approved PET and MRI imaging of core biomarkers (ATN) for AD diagnosis suffer from reliability, high cost, exceptionally sophisticated and expensive instrumentation, need for clinical expertise, radiation exposure, and low resolution. Notably, there are no approved early and differential diagnostic methods for the detection of AD in the case of mixed dementia. Over the last decade, many NIRF probes have been developed with high selectivity, sensitivity and accurate detection of different biomarkers with the potential for definitive and differential diagnosis of AD from other neurodegenerative disorders. Advancement in NIR imaging technology is not yet available for clinical use. Chemical tools for NIRF are available and the NIRF-based imaging techniques are anticipated to revolutionise AD diagnosis in the near future. The accumulation of different alloforms of Aβ and tau is associated with early and progressive stages of disease, and there is a need for developing chemical probes targeting these different alloforms. Recent and future advancements in NMR and cryo-EM to elucidate high resolution 3D structures of distinct pathologically relevant alloforms of Aβ and tau can foster the development of selective and sensitive probes. Although FDG–PET and MRI have been explored to assess neurodegeneration, they lack characteristic patterns and accuracy of diagnosis. A functional MRI technique augmented with better contrast agents is required to achieve required sensitivity. The development of an atlas encompasing the structural and functional changes occur in the AD brain at different stages of disease aid the accuracy of early diagnosis and prognosis. In addition to core biomarkers (ATN), indirect biomarkers are emerging as potential targets for early and accurate diagnosis of AD. For instance, neuroinflammation and synaptic damage are evident in advance to clinical symptoms. Although there are potential biomarkers associated with AD pathologies identified, there is ample scope to find new and potentially relevant biomarkers. There are limited chemical probes to target indirect biomarkers and there is a need to develop selective and sensitive probes that can be used in combination with core biomarkers through multiplexing and multimodal imaging and detection for

 

accurate diagnosis. Circulating biomarkers are simple and cost-effective targets for minimally or non-invasive AD diagnosis. Recently, many blood-based biomarkers are identified and validated with high diagnostic value in clinical cases. Among them, Aβ and tau biomarkers are tested in large clinical samples, which correlate with cognitive decline. These biomarkers in blood were analysed using standard ELISA and MS-based techniques. Future research must be aimed at developing simple, sensitive, and reliable chemical probes for the rapid detection of biomarkers in circulating fluids. The panel of circulating biomarkers (protein and RNA) enhances the sensitivity and specificity, through multiplexing and multimodal detection techniques. MS is a powerful technique that needs to be exploited to assess the protein and metabolite biomarker panel for accurate and early diagnosis. The multimodal imaging and multiplexed detection of various reliable biomarkers generating a signature fingerprint provide information on disease onset and progression which can be used for prognosis, early diagnosis, clinical staging and management of personalised medication (Fig. 6). AI and machine learning are highly valuable tools to develop molecular probes and signature fingerprints through integrated efforts by scientific, clinical and technology research communities.

Over three decades of therapeutics targeting Aβ yielded just one conditionally approved drug that alters the disease pathology. In recent times, tau has been explored as a potential target with mixed outputs. Many immunotherapeutics targeting both Aβ and tau are successful in preclinical and initial clinical trials. Aβ antibody therapies are facing failures due to poor cognitive improvements, while the fate of tau targeted immunotherapeutics is yet to be fully assessed in large clinical trials. There is ample scope to develop antibody-drug conjugates (ADC) to tackle complex AD pathologies. The active drug aimed at one of the disease mechanisms or targets can be conjugated with mAbs targeting another target to synergistically ameliorate complex disease pathologies. Understanding of complex pathology of AD pushed the drug research from classical Aβ and tau targeting towards other tangible targets by adopting inclusive and holistic approaches. Among them, metal dyshomeostasis oxidative stress, mitochondrial damage and neuroinflammation need special consideration. Neuroinflammation plays a major role in AD and the therapeutics developed to curb neuroinflammation are promising. The treatment of complex multifactorial AD is possible through multipronged drug development strategies that synergistically address multiple targets. In recent years, many groups are actively developing hybrid and multifunctional molecules (HMMs and MFMs) that target two or more disease aetiologies and the results are promising. Utmost care must be taken to the design of HMMs and MFMs that synergistically target multiple disease targets to manage and cure AD. These rational strategies explore small molecules, natural products and their derivatives, and hybrid conjugates to discover multifunctional drug candidates through multiplexed high throughput screening platforms to find the magic bullets for AD (Fig. 10). Advanced computational approaches including AI and machine learning are anticipated to play key roles in the design, screening, and validation of novel drug candidates. The drugs developed *in vitro* are further assessed in Tg mouse models. The development of viable 3D cell and Tg mouse models inclusive of different AD pathological aspects is necessary to test the true efficacy of HMM and MFM therapeutic candidates.[250] Over the years, several studies have showed the role of gender, ethnic and racial differences in AD pathology. AD drug discovery must take these factors into account in preclinical and clinical trials for better and personalised medication.[251] Overall, multipronged strategies targeting multiple biomarkers and targets with synergistic action are indispensable in the development of early diagnostics and potent therapeutics to tackle multifactorial AD, which in turn ease the burden on global public health and economy.

## Author contributions

TG conceived the topic and outline for the perspective. MR prepared the draft under the guidance of TG. TG and MR finalised the manuscript.

## Conflicts of interest

There are no conflicts to declare.

## Acknowledgements

The authors thank JNCASR, CEFPRA (IFCPAR/CEFIPRA-62T10-3), the Department of Science and Technology (DST), New Delhi, India, core grant (CRG/2020/004594), and Science and Engineering Research Board (SERB), New Delhi, India, and MR thanks UGC for a student fellowship and lab members for their inputs.

## References

1 *Alzheimer's disease: recent findings in pathophysiology, diagnostic and therapeutic modalities*, ed. T. Govindaraju, Royal Society Chemistry, 2021.
2 Alzheimers Association, *Alzheimer's Dementia*, 2021, **17**, 327–406.
3 B. Dubois, H. H. Feldman, C. Jacova, S. T. DeKosky, *et al.*, *Lancet Neurol.*, 2007, **6**, 734–746.
4 K. Rajasekhar, M. Chakrabarti and T. Govindaraju, *Chem. Commun.*, 2015, **51**, 13434–13450.
5 S. Samanta, M. Ramesh and T. Govindaraju, *Alzheimer's is a multifactorial disease in Alzheimer's disease: recent findings in pathophysiology, diagnostic and therapeutic modalities*, Royal Society of Chemistry, 2022, pp. 1–34.
6 P. H. Axelsen, H. Komatsu and I. V. Murray, *Physiology*, 2011, **26**, 54–69.
7 Y. Huang and L. Mucke, *Cell*, 2012, **148**, 1204–1222.
8 K. Rajasekhar and T. Govindaraju, *RSC Adv.*, 2018, **8**, 23780–23804.
9 M. Ramesh, P. Gopinath and T. Govindaraju, *ChemBioChem*, 2020, **21**, 1052–1079.
10 J. M. Long and D. M. Holtzman, *Cell*, 2019, **179**, 312–339.

11 M. A. DeTure and D. W. Dickson, *Mol. Neurodegener.*, 2019, **14**, 32.
12 C. R. Jack Jr, D. A. Bennett, K. Blennow, M. C. Carrillo, *et al.*, *Alzheimer's Dementia*, 2018, **14**, 535–562.
13 T. Lashley, J. M. Schott, P. Weston, C. E. Murray, H. Wellington, A. Keshavan, S. C. Foti, M. Foiani, J. Toombs, J. D. Rohrer, A. Heslegrave and H. Zetterberg, *Dis. Models Mech.*, 2018, **5**, 11.
14 H. Arora, M. Ramesh, K. Rajasekhar and T. Govindaraju, *Bull. Chem. Soc. Jpn.*, 2020, **93**, 507–546.
15 P. C. Ke, R. Zhou, L. C. Serpell, R. Riek, T. P. J. Knowles, H. A. Lashuel, E. Gazit, I. W. Hamley, T. P. Davis, M. Fändrich, D. E. Otzen, M. R. Chapman, C. M. Dobson, D. S. Eisenberg and R. Mezzenga, *Chem. Soc. Rev.*, 2020, **49**, 5473–5509.
16 S. Woloshin and A. S. Kesselheim, *JAMA Intern. Med.*, 2022, **182**, 892.
17 T. Mondal, S. Samanta, A. Kumar and T. Govindaraju, *Multifunctional inhibitors of multifaceted Aβ toxicity of Alzheimer's disease in Alzheimer's disease: recent findings in pathophysiology, diagnostic and therapeutic modalities*, Royal Society of Chemistry, 2022, pp. 455–486.
18 M. G. Savelieff, G. Nam, J. Kang, H. J. Lee, M. Lee and M. H. Lim, *Chem. Rev.*, 2019, **119**, 1221–1322.
19 D. Padhi and T. Govindaraju, *J. Med. Chem.*, 2022, **65**, 7088–7105.
20 C. L. Teoh, D. Su, S. Sahu, S.-W. Yun, E. Drummond, F. Prelli, S. Lim, S. Cho, S. Ham, T. Wisniewski and Y.-T. Chang, *J. Am. Chem. Soc.*, 2015, **137**, 13503–13509.
21 Y. Li, D. Xu, A. Sun, S.-L. Ho, C.-Y. Poon, H.-N. Chan, O. T. W. Ng, K. K. L. Yung, H. Yan, H.-W. Li and M. S. Wong, *Chem. Sci.*, 2017, **8**, 8279–8284.
22 J. Yang, F. Zeng, X. Li, C. Ran, Y. Xu and Y. Li, *Chem. Commun.*, 2020, **56**, 583–586.
23 K. Rajasekhar, N. Narayanaswamy, N. A. Murugan, G. Kuang, H. Ågren and T. Govindaraju, *Sci. Rep.*, 2016, **6**, 23668.
24 K. Rajasekhar, N. Narayanaswamy, N. A. Murugan, K. Viccaro, H.-G. Lee, K. Shah and T. Govindaraju, *Biosens. Bioelectron.*, 2017, **98**, 54–61.
25 W. Ren, J. Zhang, C. Peng, H. Xiang, J. Chen, C. Peng, W. Zhu, R. Huang, H. Zhang and Y. Hu, *Bioconjugate Chem.*, 2018, **29**, 3459–3466.
26 G. Lv, A. Sun, M. Wang, P. Wei, R. Li and T. Yi, *Chem. Commun.*, 2020, **56**, 1625–1628.
27 K. Zhou, H. Bai, L. Feng, J. Dai and M. Cui, *Anal. Chem.*, 2017, **89**, 9432–9437.
28 Y. Li, J. Yang, H. Liu, J. Yang, L. Du, H. Feng, Y. Tian, J. Cao and C. Ran, *Chem. Sci.*, 2017, **8**, 7710–7717.
29 J. Hatai, L. Motiei and D. Margulies, *J. Am. Chem. Soc.*, 2017, **139**, 2136–2139.
30 W. Fu, C. Yan, Z. Guo, J. Zhang, H. Zhang, H. Tian and W.-H. Zhu, *J. Am. Chem. Soc.*, 2019, **141**, 3171–3177.
31 J. Yang, W. Yin, R. Van, K. Yin, P. Wang, C. Zheng, B. Zhu, K. Ran, C. Zhang, M. Kumar, Y. Shao and C. Ran, *Nat. Commun.*, 2020, **11**, 4052.
32 K. Zhou, C. Yuan, B. Dai, K. Wang, Y. Chen, D. Ma, J. Dai, Y. Liang, H. Tan and M. Cui, *J. Med. Chem.*, 2019, **62**, 6694–6704.
33 W. E. Klunk, H. Engler, A. Nordberg, Y. Wang, *et al.*, *Ann. Neurol.*, 2004, **55**, 306–319.
34 C. Curtis, J. E. Gamez, U. Singh, C. H. Sadowsky, *et al.*, *JAMA Neurology*, 2015, **72**, 287–294.
35 O. Sabri, M. N. Sabbagh, J. Seibyl, H. Barthel, *et al.*, *Alzheimer's Dementia*, 2015, **11**, 964–974.
36 C. M. Clark, M. J. Pontecorvo, T. G. Beach, B. J. Bedell, *et al.*, *Lancet Neurol.*, 2012, **11**, 669–678.
37 T. Grimmer, K. Shi, J. Diehl-Schmid, B. Natale, A. Drzezga, S. Förster, H. Förstl, M. Schwaiger, I. Yakushev, H.-J. Wester, A. Kurz and B. H. Yousefi, *Mol. Psychiatry*, 2020, **25**, 2608–2619.
38 Y. Huang, H.-J. Cho, N. Bandara, L. Sun, D. Tran, B. E. Rogers and L. M. Mirica, *Chem. Sci.*, 2020, **11**, 7789–7799.
39 J. Yang, Y. Zaim Wadghiri, D. Minh Hoang, W. Tsui, Y. Sun, E. Chung, Y. Li, A. Wang, M. de Leon and T. Wisniewski, *NeuroImage*, 2011, **55**, 1600–1609.
40 J.-H. Kim, T. L. Ha, G. H. Im, J. Yang, S. W. Seo, J. J. Chung, S. Y. Chae, I. S. Lee and J. H. Lee, *NeuroReport*, 2014, 25.
41 A. Petiet, M. Santin, A. Bertrand, C. J. Wiggins, F. Petit, D. Houitte, P. Hantraye, J. Benavides, T. Debeir, T. Rooney and M. Dhenain, *Neurobiol. Aging*, 2012, **33**, 1533–1544.
42 M. Maruyama, H. Shimada, T. Suhara, H. Shinotoh, *et al.*, *Neuron*, 2013, **79**, 1094–1108.
43 K.-s. Park, M. K. Kim, Y. Seo, T. Ha, K. Yoo, S. J. Hyeon, Y. J. Hwang, J. Lee, H. Ryu, H. Choo and Y. Chong, *ACS Chem. Neurosci.*, 2017, **8**, 2124–2131.
44 S. Lim, M. M. Haque, D. Su, D. Kim, J.-S. Lee, Y.-T. Chang and Y. K. Kim, *Chem. Commun.*, 2017, **53**, 1607–1610.
45 P. Verwilst, H.-R. Kim, J. Seo, N.-W. Sohn, S.-Y. Cha, Y. Kim, S. Maeng, J.-W. Shin, J. H. Kwak, C. Kang and J. S. Kim, *J. Am. Chem. Soc.*, 2017, **139**, 13393–13403.
46 Y. Chen, C. Yuan, T. Xie, Y. Li, B. Dai, K. Zhou, Y. Liang, J. Dai, H. Tan and M. Cui, *Chem. Commun.*, 2020, **56**, 7269–7272.
47 A. A. Elbatrawy, S. J. Hyeon, N. Yue, E. E. A. Osman, S. H. Choi, S. Lim, Y. K. Kim, H. Ryu, M. Cui and G. Nam, *ACS Sens.*, 2021, **6**, 2281–2289.
48 Y. Zhao, O. Tietz, W.-L. Kuan, A. K. Haji-Dheere, S. Thompson, B. Vallin, E. Ronchi, G. Tóth, D. Klenerman and F. I. Aigbirhio, *Chem. Sci.*, 2020, **11**, 4773–4778.
49 T. J. Betthauser, P. J. Lao, D. Murali, T. E. Barnhart, S. Furumoto, N. Okamura, C. K. Stone, S. C. Johnson and B. T. Christian, *J. Nucl. Med.*, 2017, **58**, 996–1002.
50 L. Passamonti, P. Vázquez Rodríguez, Y. T. Hong, K. S. J. Allinson, *et al.*, *Brain*, 2017, **140**, 781–791.
51 L. Declercq, F. Rombouts, M. Koole, K. Fierens, J. Mariën, X. Langlois, J. I. Andrés, M. Schmidt, G. Macdonald, D. Moechars, W. Vanduffel, T. Tousseyn, R. Vandenberghe, K. Van Laere, A. Verbruggen and G. Bormans, *J. Nucl. Med.*, 2017, **58**, 975–981.

52 S. Sanabria Bohórquez, J. Marik, A. Ogasawara, J. N. Tinianow, *et al.*, *Eur. J. Nucl. Med. Mol. Imaging*, 2019, **46**, 2077–2089.
53 A. Mueller, S. Bullich, O. Barret, J. Madonia, *et al.*, *J. Nucl. Med.*, 2020, **61**, 911–919.
54 D. Yanagisawa, N. F. Ibrahim, H. Taguchi, S. Morikawa, T. Kato, K. Hirao, N. Shirai, T. Sogabe and I. Tooyama, *J. Neurosci. Res.*, 2018, **96**, 841–851.
55 A. Badachhape, P. A. Parekh, Q. Mu, R. Bhavane, M. Srivastava, I. Stupin, P. Bhandari, L. Devkota, E. Tanifum, K. Ghaghada and A. Annapragada, *Alzheimer's Dementia*, 2020, **16**, e041080.
56 P. Parekh, Q. Mu, A. Badachhape, R. Bhavane, M. Srivastava, L. Devkota, X. Sun, P. Bhandari, J. L. Eriksen, E. Tanifum, K. Ghaghada and A. Annapragada, *Theranostics*, 2022, **12**, 5504–5521.
57 L. Mosconi, W. H. Tsui, K. Herholz, A. Pupi, *et al.*, *J. Nucl. Med.*, 2008, **49**, 390–398.
58 L. M. Bloudek, D. E. Spackman, M. Blankenburg and S. D. Sullivan, *J. Alzheimer's Dis.*, 2011, **26**, 627–645.
59 Y.-N. Ou, W. Xu, J.-Q. Li, Y. Guo, M. Cui, K.-L. Chen, Y.-Y. Huang, Q. Dong, L. Tan and J.-T. Yu, *Alzheimer's Res. Ther.*, 2019, **11**, 57.
60 P. J. Nestor, D. Altomare, C. Festari, A. Drzezga, *et al.*, *Eur. J. Nucl. Med. Mol. Imaging*, 2018, **45**, 1509–1525.
61 I. Kilimann, M. Grothe, H. Heinsen, E. J. L. Alho, *et al.*, *J. Alzheimer's Dis.*, 2014, **40**, 687–700.
62 M. Nesteruk, T. Nesteruk, M. Styczyńska, A. Barczak, M. Mandecka, J. Walecki and M. Barcikowska-Kotowicz, *Neurol. Neurochir. Pol.*, 2015, **49**, 349–353.
63 S. Delli Pizzi, R. Franciotti, G. Bubbico, A. Thomas, M. Onofrj and L. Bonanni, *Neurobiol. Aging*, 2016, **40**, 103–109.
64 J. S. Damoiseaux, K. E. Prater, B. L. Miller and M. D. Greicius, *Neurobiol. Aging*, 2012, **33**, 828.e819–828.e830.
65 E. Yu, Z. Liao, D. Mao, Q. Zhang, G. Ji, Y. Li and Z. Ding, *Curr. Alzheimer Res.*, 2017, **14**, 628–635.
66 R. Zhou, B. Ji, Y. Kong, L. Qin, W. Ren, Y. Guan and R. Ni, *Front. Immunol.*, 2021, **12**, 739130.
67 P. Parbo, R. Ismail, K. V. Hansen, A. Amidi, *et al.*, *Brain*, 2017, **140**, 2002–2011.
68 M. Dani, M. Wood, R. Mizoguchi, Z. Fan, Z. Walker, R. Morgan, R. Hinz, M. Biju, T. Kuruvilla, D. J. Brooks and P. Edison, *Brain*, 2018, **141**, 2740–2754.
69 S. J. Finnema, N. B. Nabulsi, T. Eid, K. Detyniecki, S.-f. Lin, M.-K. Chen, R. Dhaher, D. Matuskey, E. Baum, D. Holden, D. D. Spencer, J. Mercier, J. Hannestad, Y. Huang and R. E. Carson, *Sci. Transl. Med.*, 2016, **8**, 348ra396.
70 C. Bastin, M. A. Bahri, F. Meyer, M. Manard, E. Delhaye, A. Plenevaux, G. Becker, A. Seret, C. Mella, F. Giacomelli, C. Degueldre, E. Balteau, A. Luxen and E. Salmon, *Eur. J. Nucl. Med. Mol. Imaging*, 2020, **47**, 390–402.
71 M. Naganawa, S. Li, N. Nabulsi, S. Henry, M.-Q. Zheng, R. Pracitto, Z. Cai, H. Gao, M. Kapinos, D. Labaree, D. Matuskey, Y. Huang and R. E. Carson, *J. Nucl. Med.*, 2021, **62**, 561–567.
72 Z. Cai, L. Drake, M. Naganawa, S. Najafzadeh, *et al.*, *J. Nucl. Med.*, 2020, **61**, 462.
73 S. Samanta and T. Govindaraju, *ACS Chem. Neurosci.*, 2019, **10**, 4847–4853.
74 Y. Liu, M. Nguyen, A. Robert and B. Meunier, *Acc. Chem. Res.*, 2019, **52**, 2026–2035.
75 S. A. Virk and G. D. Eslick, *J. Alzheimer's Dis.*, 2015, **47**, 629–638.
76 A. Damulina, L. Pirpamer, M. Soellradl, M. Sackl, C. Tinauer, E. Hofer, C. Enzinger, B. Gesierich, M. Duering, S. Ropele, R. Schmidt and C. Langkammer, *Radiology*, 2020, **296**, 619–626.
77 J. B. Torres, E. M. Andreozzi, J. T. Dunn, M. Siddique, I. Szanda, D. R. Howlett, K. Sunassee and P. J. Blower, *J. Nucl. Med.*, 2016, **57**, 109–114.
78 D. Maity, A. K. Manna, D. Karthigeyan, T. K. Kundu, S. K. Pati and T. Govindaraju, *Chem.–Eur. J.*, 2011, **17**, 11152–11161.
79 D. Maity, D. Karthigeyan, T. K. Kundu and T. Govindaraju, *Sens. Actuators, B*, 2013, **176**, 831–837.
80 L. Wang, Y.-L. Yin, X.-Z. Liu, P. Shen, Y.-G. Zheng, X.-R. Lan, C.-B. Lu and J.-Z. Wang, *Transl. Neurodegener.*, 2020, **9**, 10.
81 D. Maity and T. Govindaraju, *Chem. Commun.*, 2012, **48**, 1039–1041.
82 N. Narayanaswamy and T. Govindaraju, *Sens. Actuators, B*, 2012, **161**, 304–310.
83 D. Maity and T. Govindaraju, *Eur. J. Inorg. Chem.*, 2011, **2011**, 5479–5485.
84 D. Maity, V. Kumar and T. Govindaraju, *Org. Lett.*, 2012, **14**, 6008–6011.
85 D. Maity and T. Govindaraju, *Inorg. Chem.*, 2010, **49**, 7229–7231.
86 J. M. Jung, J. H. Kang, J. Han, H. Lee, M. H. Lim, K. T. Kim and C. Kim, *Sens. Actuators, B*, 2018, **267**, 58–69.
87 J. B. Chae, D. Yun, S. Kim, H. Lee, M. Kim, M. H. Lim, K. T. Kim and C. Kim, *Spectrochim. Acta, Part A*, 2019, **219**, 74–82.
88 M. Yang, S. C. Lee, M. Kim, M. H. Lim and C. Kim, *Spectrochim. Acta, Part A*, 2021, **245**, 118899.
89 T. O. Klyucherev, P. Olszewski, A. A. Shalimova, V. N. Chubarev, V. V. Tarasov, M. M. Attwood, S. Syvänen and H. B. Schiöth, *Transl. Neurodegener.*, 2022, **11**, 25.
90 S. Nagaraj, M. Ramesh and T. Govindaraju, *Circulating biomarkers for the diagnosis of Alzheimer's disease in Alzheimer's disease: recent findings in pathophysiology, diagnostic and therapeutic modalities*, Royal Society of Chemistry, 2022, pp. 415–441.
91 K.-Y. Tzen, S.-Y. Yang, T.-F. Chen, T.-W. Cheng, H.-E. Horng, H.-P. Wen, Y.-Y. Huang, C.-Y. Shiue and M.-J. Chiu, *ACS Chem. Neurosci.*, 2014, **5**, 830–836.
92 A. Nakamura, N. Kaneko, V. L. Villemagne, T. Kato, *et al.*, *Nature*, 2018, **554**, 249–254.
93 V. Pérez-Grijalba, J. Arbizu, J. Romero, E. Prieto, *et al.*, *Alzheimer's Res. Ther.*, 2019, **11**, 96.
94 S. Fossati, J. Ramos Cejudo, L. Debure, E. Pirraglia, J. Y. Sone, Y. Li, J. Chen, T. Butler, H. Zetterberg,

K. Blennow and M. J. de Leon, *Alzheimer's Dementia*, 2019, **11**, 483–492.
95 S. Janelidze, N. Mattsson, S. Palmqvist, R. Smith, *et al.*, *Nat. Med.*, 2020, **26**, 379–386.
96 N. R. Barthélemy, R. J. Bateman, C. Hirtz, P. Marin, F. Becher, C. Sato, A. Gabelle and S. Lehmann, *Alzheimer's Res. Ther.*, 2020, **12**, 26.
97 S. Janelidze, D. Berron, R. Smith, O. Strandberg, N. K. Proctor, J. L. Dage, E. Stomrud, S. Palmqvist, N. Mattsson-Carlgren and O. Hansson, *JAMA Neurology*, 2021, **78**, 149–156.
98 E. H. Thijssen, R. La Joie, A. Strom, C. Fonseca, *et al.*, *Lancet Neurol.*, 2021, **20**, 739–752.
99 N. J. Ashton, T. A. Pascoal, T. K. Karikari, A. L. Benedet, *et al.*, *Acta Neuropathol.*, 2021, **141**, 709–724.
100 R. Tarawneh, G. D'Angelo, D. Crimmins, E. Herries, T. Griest, A. M. Fagan, G. J. Zipfel, J. H. Ladenson, J. C. Morris and D. M. Holtzman, *JAMA Neurology*, 2016, **73**, 561–571.
101 E. A. J. Willemse, A. Sieben, C. Somers, Y. Vermeiren, N. De Roeck, M. Timmers, C. Van Broeckhoven, B. De Vil, P. Cras, P. P. De Deyn, J.-J. Martin, C. E. Teunissen, S. Engelborghs and M. Bjerke, *Neurobiol. Aging*, 2021, **108**, 99–109.
102 A. Öhrfelt, A. Brinkmalm, J. Dumurgier, G. Brinkmalm, O. Hansson, H. Zetterberg, E. Bouaziz-Amar, J. Hugon, C. Paquet and K. Blennow, *Alzheimer's Res. Ther.*, 2016, **8**, 41.
103 E. Morenas-Rodríguez, Y. Li, B. Nuscher, N. Franzmeier, *et al.*, *Lancet Neurol.*, 2022, **21**, 329–341.
104 A. Vergallo, S. Lista, P. Lemercier, P. A. Chiesa, *et al.*, *Neurobiol. Aging*, 2020, **96**, 22–32.
105 K. Wilczyńska, M. Maciejczyk, A. Zalewska and N. Waszkiewicz, *Front. Psychiatry*, 2021, **12**, 725511.
106 O. Preische, S. A. Schultz, A. Apel, J. Kuhle, *et al.*, *Nat. Med.*, 2019, **25**, 277–283.
107 N. J. Ashton, S. Janelidze, A. Al Khleifat, A. Leuzy, *et al.*, *Nat. Commun.*, 2021, **12**, 3400.
108 M. Babić Leko, F. Borovečki, N. Dejanović, P. R. Hof and G. Šimić, *J. Alzheimer's Dis.*, 2016, **50**, 765–778.
109 L. Feng, Y.-T. Liao, J.-C. He, C.-L. Xie, S.-Y. Chen, H.-H. Fan, Z.-P. Su and Z. Wang, *BMC Neurol.*, 2018, **18**, 4.
110 G. Lugli, A. M. Cohen, D. A. Bennett, R. C. Shah, C. J. Fields, A. G. Hernandez and N. R. Smalheiser, *PLoS One*, 2015, **10**, e0139233.
111 S. Nagaraj, K. Laskowska-Kaszub, K. J. Dębski, J. Wojsiat, M. Dąbrowski, T. Gabryelewicz, J. Kuźnicki and U. Wojda, *Oncotarget*, 2017, **8**, 16122–16143.
112 J. T. Wiedrick, J. I. Phillips, T. A. Lusardi, T. J. McFarland, B. Lind, U. S. Sandau, C. A. Harrington, J. A. Lapidus, D. R. Galasko, J. F. Quinn and J. A. Saugstad, *J. Alzheimer's Dis.*, 2019, **67**, 875–891.
113 J. D. Doecke, S. M. Laws, N. G. Faux, W. Wilson, *et al.*, *Arch. Neurol.*, 2012, **69**, 1318–1325.
114 N. C. Cullen, A. Leuzy, S. Janelidze, S. Palmqvist, A. L. Svenningsson, E. Stomrud, J. L. Dage, N. Mattsson-Carlgren and O. Hansson, *Nat. Commun.*, 2021, **12**, 3555.
115 M. Milà-Alomà, A. Brinkmalm, N. J. Ashton, H. Kvartsberg, *et al.*, *Neurology*, 2021, **97**, e2065–e2078.
116 L. Jia, M. Zhu, C. Kong, Y. Pang, H. Zhang, Q. Qiu, C. Wei, Y. Tang, Q. Wang, Y. Li, T. Li, F. Li, Q. Wang, Y. Li, Y. Wei and J. Jia, *Alzheimer's Dementia*, 2021, **17**, 49–60.
117 V. R. Varma, A. M. Oommen, S. Varma, R. Casanova, *et al.*, *PLoS Med.*, 2018, **15**, e1002482.
118 M. N. Sabbagh, J. Shi, M. Lee, L. Arnold, Y. Al-Hasan, J. Heim and P. McGeer, *BMC Neurol.*, 2018, **18**, 155.
119 M. Shi, Y.-T. Sui, E. R. Peskind, G. Li, H. Hwang, I. Devic, C. Ginghina, J. S. Edgar, C. Pan, D. R. Goodlett, A. R. Furay, L. F. Gonzalez-Cuyar and J. Zhang, *J. Alzheimer's Dis.*, 2011, **27**, 299–305.
120 H. Pekeles, H. Y. Qureshi, H. K. Paudel, H. M. Schipper, M. Gornistky and H. Chertkow, *Alzheimer's Dementia*, 2018, **10**, 53–60.
121 E. Carro, F. Bartolomé, F. Bermejo-Pareja, A. Villarejo-Galende, J. A. Molina, P. Ortiz, M. Calero, A. Rabano, J. L. Cantero and G. Orive, *Alzheimer's Dementia*, 2017, **8**, 131–138.
122 M. Ramesh and T. Govindaraju, *Lactoferrin: a potential theranostic candidate for Alzheimer's disease in Alzheimer's disease: recent findings in pathophysiology, diagnostic and therapeutic modalities*, Royal Society of Chemistry, 2022, pp. 442–454.
123 H. S. Gleerup, C. S. Jensen, P. Høgh, S. G. Hasselbalch and A. H. Simonsen, *EBioMedicine*, 2021, **67**, 103361.
124 G. Kalló, M. Emri, Z. Varga, B. Ujhelyi, J. Tőzsér, A. Csutak and É. Csősz, *PLoS One*, 2016, **11**, e0158000.
125 F. Yao, X. Hong, S. Li, Y. Zhang, Q. Zhao, W. Du, Y. Wang and J. Ni, *J. Alzheimer's Dis.*, 2018, **65**, 421–431.
126 M. Ramesh, S. Samanta and T. Govindaraju, *Molecular probes for the diagnosis of Alzheimer's disease with implications for multiplexed and multimodal strategies in Alzheimer's disease: recent findings in pathophysiology, diagnostic and therapeutic modalities*, Royal Society of Chemistry, 2022, pp. 377–414.
127 J. S. Birks, *Cochrane Database of Systematic Reviews*, 2006, **1**, CD005593.
128 G. Marucci, M. Buccioni, D. D. Ben, C. Lambertucci, R. Volpini and F. Amenta, *Neuropharmacology*, 2021, **190**, 108352.
129 F. Amenta, S. K. Tayebati, D. Vitali and M. A. Di Tullio, *Mech. Ageing Dev.*, 2006, **127**, 173–179.
130 F. Amenta, A. Carotenuto, A. M. Fasanaro, R. Rea and E. Traini, *J. Alzheimer's Dis.*, 2014, **42**, S281–S288.
131 A. Carotenuto, A. M. Fasanaro, V. Manzo, F. Amenta and E. Traini, *Journal of Alzheimer's Disease Reports*, 2022, **6**, 235–243.
132 E. McDade, I. Voytyuk, P. Aisen, R. J. Bateman, M. C. Carrillo, B. De Strooper, C. Haass, E. M. Reiman, R. Sperling, P. N. Tariot, R. Yan, C. L. Masters, R. Vassar and S. F. Lichtenthaler, *Nat. Rev. Neurol.*, 2021, **17**, 703–714.
133 U. Neumann, M. Ufer, L. H. Jacobson, M.-L. Rouzade-Dominguez, *et al.*, *EMBO Mol. Med.*, 2018, **10**, e9316.
134 J. E. Luo and Y.-M. Li, *Cell Biosci.*, 2022, **12**, 2.

135 B. Vellas, O. Sol, P. J. Snyder, P. J. Ousset, R. Haddad, M. Maurin, J. C. Lemarie, L. Desire and M. P. Pando, *Curr. Alzheimer Res.*, 2011, **8**, 203–212.
136 K. Endres, F. Fahrenholz, J. Lotz, C. Hiemke, S. Teipel, K. Lieb, O. Tüscher and A. Fellgiebel, *Neurology*, 2014, **83**, 1930–1935.
137 Study of APH-1105 in Patients with Mild to Moderate Alzheimer's Disease, ClinicalTrials.gov identifier: NCT03806478, Updated July 27, 2021, **https://clinicaltrials.gov/ct2/show/NCT03806478**.
138 Y. Y. Syed, *Drugs*, 2020, **80**, 441–444.
139 S. Samanta, M. Ramesh, A. Kumar and T. Govindaraju, *The role of gut microbiome in Alzheimer's disease and therapeutic strategies in Alzheimer's disease: recent findings in pathophysiology, diagnostic and therapeutic modalities*, Royal Society of Chemistry, 2022, pp. 354–376.
140 K. Rajasekhar, K. Mehta and T. Govindaraju, *ACS Chem. Neurosci.*, 2018, **9**, 1432–1440.
141 C. Soto, E. M. Sigurdsson, L. Morelli, R. Asok Kumar, E. M. Castaño and B. Frangione, *Nat. Med.*, 1998, **4**, 822–826.
142 L. O. Tjernberg, J. Näslund, F. Lindqvist, J. Johansson, A. R. Karlström, J. Thyberg, L. Terenius and C. Nordstedt, *J. Biol. Chem.*, 1996, **271**, 8545–8548.
143 K. Rajasekhar, S. N. Suresh, R. Manjithaya and T. Govindaraju, *Sci. Rep.*, 2015, **5**, 8139.
144 K. Rajasekhar, C. Madhu and T. Govindaraju, *ACS Chem. Neurosci.*, 2016, **7**, 1300–1310.
145 S. Pellegrino, N. Tonali, E. Erba, J. Kaffy, M. Taverna, A. Contini, M. Taylor, D. Allsop, M. L. Gelmi and S. Ongeri, *Chem. Sci.*, 2017, **8**, 1295–1302.
146 S. L. Griner, P. Seidler, J. Bowler, K. A. Murray, T. P. Yang, S. Sahay, M. R. Sawaya, D. Cascio, J. A. Rodriguez, S. Philipp, J. Sosna, C. G. Glabe, T. Gonen and D. S. Eisenberg, *eLife*, 2019, **8**, e46924.
147 M. Konar, D. Ghosh, S. Samanta and T. Govindaraju, *RSC Chem. Biol.*, 2022, **3**, 220–226.
148 C. Madhu, C. Voshavar, K. Rajasekhar and T. Govindaraju, *Org. Biomol. Chem.*, 2017, **15**, 3170–3174.
149 C. Balachandra, D. Padhi and T. Govindaraju, *ChemMedChem*, 2021, **16**, 2558–2587.
150 S. Samanta, K. Rajasekhar, M. Ramesh, N. A. Murugan, S. Alam, D. Shah, J. P. Clement and T. Govindaraju, *Adv. Ther.*, 2021, **4**, 2000225.
151 C. Holmes, D. Boche, D. Wilkinson, G. Yadegarfar, V. Hopkins, A. Bayer, R. W. Jones, R. Bullock, S. Love, J. W. Neal, E. Zotova and J. A. R. Nicoll, *Lancet*, 2008, **372**, 216–223.
152 F. Pasquier, C. Sadowsky, A. Holstein, G. L. P. Leterme, Y. Peng, N. Jackson, N. C. Fox, N. Ketter, E. Liu, J. M. Ryan and ACC-001 (QS-21) Study Team, *J. Alzheimer's Dis.*, 2016, **51**, 1131–1143.
153 M. R. Farlow, N. Andreasen, M.-E. Riviere, I. Vostiar, A. Vitaliti, J. Sovago, A. Caputo, B. Winblad and A. Graf, *Alzheimer's Res. Ther.*, 2015, **7**, 23.
154 S. Salloway, R. Sperling, N. C. Fox, K. Blennow, W. Klunk, M. Raskind, M. Sabbagh, L. S. Honig, A. P. Porsteinsson, S. Ferris, M. Reichert, N. Ketter, B. Nejadnik, V. Guenzler, M. Miloslavsky, D. Wang, Y. Lu, J. Lull, I. C. Tudor, E. Liu, M. Grundman, E. Yuen, R. Black and H. R. Brashear, *N. Engl. J. Med.*, 2014, **370**, 322–333.
155 L. S. Honig, B. Vellas, M. Woodward, M. Boada, *et al.*, *N. Engl. J. Med.*, 2018, **378**, 321–330.
156 S. Ostrowitzki, R. A. Lasser, E. Dorflinger, P. Scheltens, *et al.*, *Alzheimer's Res. Ther.*, 2017, **9**, 95.
157 H. Guthrie, L. S. Honig, H. Lin, K. M. Sink, K. Blondeau, A. Quartino, M. Dolton, M. Carrasco-Triguero, Q. Lian, T. Bittner, D. Clayton, J. Smith and S. Ostrowitzki, *J. Alzheimer's Dis.*, 2020, **76**, 967–979.
158 S. Budd Haeberlein, J. O'Gorman, P. Chiao, T. Bussière, P. von Rosenstiel, Y. Tian, Y. Zhu, C. von Hehn, S. Gheuens, L. Skordos, T. Chen and A. Sandrock, *Journal of Prevention of Alzheimer's Disease*, 2017, **4**, 255–263.
159 C. Hureau, *Role of metal ions in Alzheimer's disease: mechanistic aspects contributing to neurotoxicity in Alzheimer's disease: recent findings in pathophysiology, diagnostic and therapeutic modalities*, Royal Society of Chemistry, 2022, pp. 170–192.
160 Y.-H. Zhang, J. Raymick, S. Sarkar, D. K. Lahiri, B. Ray, D. Holtzman, M. Dumas and L. C. Schmued, *Curr. Alzheimer Res.*, 2013, **10**, 494–506.
161 A. I. Bush and R. E. Tanzi, *Neurotherapeutics*, 2008, **5**, 421–432.
162 S.-J. Hyung, A. S. DeToma, J. R. Brender, S. Lee, S. Vivekanandan, A. Kochi, J.-S. Choi, A. Ramamoorthy, B. T. Ruotolo and M. H. Lim, *Proc. Natl. Acad. Sci. U. S. A.*, 2013, **110**, 3743–3748.
163 J.-Y. Lee, J. E. Friedman, I. Angel, A. Kozak and J.-Y. Koh, *Neurobiol. Aging*, 2004, **25**, 1315–1321.
164 S. S. Hindo, A. M. Mancino, J. J. Braymer, Y. Liu, S. Vivekanandan, A. Ramamoorthy and M. H. Lim, *J. Am. Chem. Soc.*, 2009, **131**, 16663–16665.
165 S. Xie, J. Chen, X. Li, T. Su, Y. Wang, Z. Wang, L. Huang and X. Li, *Bioorg. Med. Chem.*, 2015, **23**, 3722–3729.
166 K. Rajasekhar, S. Samanta, V. Bagoband, N. A. Murugan and T. Govindaraju, *iScience*, 2020, **23**, 101005.
167 D. Padhi, M. Ramesh and T. Govindaraju, *Post-translational modifications and Alzheimer's disease in Alzheimer's disease: recent findings in pathophysiology, diagnostic and therapeutic modalities*, Royal Society of Chemistry, 2022, pp. 255–286.
168 S. Lovestone, M. Boada, B. Dubois, M. Hüll, J. O. Rinne, H.-J. Huppertz, M. Calero, M. V. Andrés, B. Gómez-Carrillo, T. León, T. del Ser and ARGO investigators, *J. Alzheimer's Dis.*, 2015, **45**, 75–88.
169 C. H. van Dyck, H. B. Nygaard, K. Chen, M. C. Donohue, *et al.*, *JAMA Neurology*, 2019, **76**, 1219–1229.
170 X. Zhang, I. Hernandez, D. Rei, W. Mair, J. K. Laha, M. E. Cornwell, G. D. Cuny, L.-H. Tsai, J. A. J. Steen and K. S. Kosik, *J. Biol. Chem.*, 2013, **288**, 22042–22056.
171 X. Dou, H. Huang, Y. Li, L. Jiang, Y. Wang, H. Jin, N. Jiao, L. Zhang, L. Zhang and Z. Liu, *J. Med. Chem.*, 2019, **62**, 6645–6664.

172 X.-L. Wang, Y. Xiong, Y. Yang, Q.-z. Tuo, X.-c. Wang, R. Chen, Q. Tian, Z.-p. Zhang, X. Yan, Z.-y. Yang, J.-Z. Wang and R. Liu, *Eur. J. Pharmacol.*, 2015, **754**, 134–139.
173 T.-T. Chu, N. Gao, Q.-Q. Li, P.-G. Chen, X.-F. Yang, Y.-X. Chen, Y.-F. Zhao and Y.-M. Li, *Cell Chem. Biol.*, 2016, **23**, 453–461.
174 B. Zhang, J. Carroll, J. Q. Trojanowski, Y. Yao, M. Iba, J. S. Potuzak, A.-M. L. Hogan, S. X. Xie, C. Ballatore, A. B. Smith, V. M.-Y. Lee and K. R. Brunden, *J. Neurosci.*, 2012, **32**, 3601–3611.
175 R. M. Tsai, Z. Miller, M. Koestler, J. C. Rojas, *et al.*, *JAMA Neurology*, 2020, **77**, 215–224.
176 P. Gopinath, M. Ramesh and T. Govindaraju, *Tau-targeting therapeutic strategies for Alzheimer's disease in Alzheimer's disease: recent findings in pathophysiology, diagnostic and therapeutic modalities*, Royal Society of Chemistry, 2022, pp. 487–514.
177 G. K. Wilcock, S. Gauthier, G. B. Frisoni, J. Jia, *et al.*, *J. Alzheimer's Dis.*, 2018, **61**, 435–457.
178 T. Silva, T. Mohamed, A. Shakeri, P. P. N. Rao, P. Soares da Silva, F. Remião and F. Borges, *Eur. J. Med. Chem.*, 2019, **167**, 146–152.
179 A. Paul, G. K. Viswanathan, A. Huber, E. Arad, H. Engel, R. Jelinek, E. Gazit and D. Segal, *FEBS J.*, 2021, **288**, 4267–4290.
180 M. Ramesh, A. Acharya, N. A. Murugan, H. Ila and T. Govindaraju, *ChemBioChem*, 2021, **22**, 3348–3357.
181 S. A. Sievers, J. Karanicolas, H. W. Chang, A. Zhao, L. Jiang, O. Zirafi, J. T. Stevens, J. Münch, D. Baker and D. Eisenberg, *Nature*, 2011, **475**, 96–100.
182 J. Zheng, C. Liu, M. R. Sawaya, B. Vadla, S. Khan, R. J. Woods, D. Eisenberg, W. J. Goux and J. S. Nowick, *J. Am. Chem. Soc.*, 2011, **133**, 3144–3157.
183 P. M. Seidler, D. R. Boyer, J. A. Rodriguez, M. R. Sawaya, D. Cascio, K. Murray, T. Gonen and D. S. Eisenberg, *Nat. Chem.*, 2018, **10**, 170–176.
184 N. V. Gorantla, L. P. Sunny, K. Rajasekhar, P. G. Nagaraju, P. P. Cg, T. Govindaraju and S. Chinnathambi, *ACS Omega*, 2021, **6**, 11131–11138.
185 E. Kontsekova, N. Zilka, B. Kovacech, P. Novak and M. Novak, *Alzheimer's Res. Ther.*, 2014, **6**, 44.
186 P. Novak, B. Kovacech, S. Katina, R. Schmidt, *et al.*, *Nature Aging*, 2021, **1**, 521–534.
187 H. Rajamohamedsait, S. Rasool, W. Rajamohamedsait, Y. Lin and E. M. Sigurdsson, *Sci. Rep.*, 2017, **7**, 17034.
188 H. Davtyan, W. W. Chen, K. Zagorski, J. Davis, I. Petrushina, K. Kazarian, D. H. Cribbs, M. G. Agadjanyan, M. Blurton-Jones and A. Ghochikyan, *Vaccine*, 2017, **35**, 2015–2024.
189 T. West, Y. Hu, P. B. Verghese, R. J. Bateman, J. B. Braunstein, I. Fogelman, K. Budur, H. Florian, N. Mendonca and D. M. Holtzman, *Journal of Prevention of Alzheimer's Disease*, 2017, **4**, 236–241.
190 A. L. Boxer, I. Qureshi, M. Ahlijanian, M. Grundman, *et al.*, *Lancet Neurol.*, 2019, **18**, 549–558.
191 T. Umeda, H. Eguchi, Y. Kunori, Y. Matsumoto, T. Taniguchi, H. Mori and T. Tomiyama, *Ann. Clin. Transl. Neurol.*, 2015, **2**, 241–255.
192 C.-l. Dai, Y. C. Tung, F. Liu, C.-X. Gong and K. Iqbal, *Alzheimer's Res. Ther.*, 2017, **9**, 1.
193 V. Corsetti, A. Borreca, V. Latina, G. Giacovazzo, *et al.*, *Brain Commun.*, 2020, **2**, fcaa039.
194 M. Roberts, I. Sevastou, Y. Imaizumi, K. Mistry, *et al.*, *Acta Neuropathol. Commun.*, 2020, **8**, 13.
195 A. S. Pithadia and M. H. Lim, *Curr. Opin. Chem. Biol.*, 2012, **16**, 67–73.
196 R. J. Kryscio, E. L. Abner, A. Caban-Holt, M. Lovell, P. Goodman, A. K. Darke, M. Yee, J. Crowley and F. A. Schmitt, *JAMA Neurology*, 2017, **74**, 567–573.
197 G. Garg, S. Singh, A. K. Singh and S. I. Rizvi, *Can. J. Physiol. Pharmacol.*, 2018, **96**, 1189–1196.
198 T. M. Holland, P. Agarwal, Y. Wang, S. E. Leurgans, D. A. Bennett, S. L. Booth and M. C. Morris, *Neurology*, 2020, **94**, e1749–e1756.
199 C. Sawda, C. Moussa and R. S. Turner, *Ann. N. Y. Acad. Sci.*, 2017, **1403**, 142–149.
200 S. Singh, A. K. Singh, G. Garg and S. I. Rizvi, *Life Sci.*, 2018, **193**, 171–179.
201 F. Zhao, J. Zhang and N. Chang, *Eur. J. Pharmacol.*, 2018, **824**, 1–10.
202 F. Morroni, G. Sita, A. Graziosi, E. Turrini, C. Fimognari, A. Tarozzi and P. Hrelia, *Aging Dis.*, 2018, **9**, 605–622.
203 S. Samanta, K. Rajasekhar, V. Babagond and T. Govindaraju, *ACS Chem. Neurosci.*, 2019, **10**, 3611–3621.
204 M. J. McManus, M. P. Murphy and J. L. Franklin, *J. Neurosci.*, 2011, **31**, 15703–15715.
205 M. Ramesh, K. Rajasekhar, K. Gupta, V. Babagond, D. K. Saini and T. Govindaraju, *Org. Biomol. Chem.*, 2021, **19**, 801–808.
206 J. Goldberg, A. Currais, M. Prior, W. Fischer, C. Chiruta, E. Ratliff, D. Daugherty, R. Dargusch, K. Finley, P. B. Esparza-Moltó, J. M. Cuezva, P. Maher, M. Petrascheck and D. Schubert, *Aging Cell*, 2018, **17**, e12715.
207 X. Zhu, G. Perry, M. A. Smith and X. Wang, *J. Alzheimer's Dis.*, 2013, **33**, S253–S262.
208 P. H. Reddy, M. Manczak and R. Kandimalla, *Hum. Mol. Genet.*, 2017, **26**, 1483–1496.
209 T. Ahmed, S. Javed, S. Javed, A. Tariq, D. Šamec, S. Tejada, S. F. Nabavi, N. Braidy and S. M. Nabavi, *Mol. Neurobiol.*, 2017, **54**, 2622–2635.
210 A. U. Joshi, N. L. Saw, M. Shamloo and D. Mochly-Rosen, *Oncotarget*, 2018, **9**, 6128–6143.
211 L. Zhang, S. Zhang, I. Maezawa, S. Trushin, P. Minhas, M. Pinto, L. W. Jin, K. Prasain, T. D. Nguyen, Y. Yamazaki, T. Kanekiyo, G. Bu, B. Gateno, K. O. Chang, K. A. Nath, E. Nemutlu, P. Dzeja, Y. P. Pang, D. H. Hua and E. Trushina, *EBioMedicine*, 2015, **2**, 294–305.
212 D. A. Ryskamp, S. Korban, V. Zhemkov, N. Kraskovskaya and I. Bezprozvanny, *Front. Neurosci.*, 2019, **13**, 862.
213 S. Macfarlane, M. Cecchi, D. Moore, P. Maruff, T. Zografidis and C. Missling, *Alzheimer's Dementia*, 2016, **12**, P1174.
214 E. F. Fang, Y. Hou, K. Palikaras, B. A. Adriaanse, *et al.*, *Nat. Neurosci.*, 2019, **22**, 401–412.

215 D. V. Hansen, B. K. Cullimore, J. C. Johanson and W. Cheng, *Microglial blockade of the amyloid cascade: a new therapeutic frontier in Alzheimer's disease: recent findings in pathophysiology, diagnostic and therapeutic modalities*, Royal Society of Chemistry, 2022, pp. 193–254.
216 J. Wang, L. Tan, H. F. Wang, C. C. Tan, X. F. Meng, C. Wang, S. W. Tang and J. T. Yu, *J. Alzheimer's Dis.*, 2015, **44**, 385–396.
217 H. Potter, J. H. Woodcock, T. D. Boyd, C. M. Coughlan, *et al.*, *Alzheimer's Dementia*, 2021, **7**, e12158.
218 N. Torika, K. Asraf, R. N. Apte and S. Fleisher-Berkovich, *CNS Neurosci. Ther.*, 2018, **24**, 231–242.
219 N. Torika, K. Asraf, H. Cohen and S. Fleisher-Berkovich, *Brain, Behav., Immun.*, 2017, **64**, 80–90.
220 Study Evaluating Safety, Tolerability, and PK of Multiple Ascending Doses of GC021109 in Subjects with Mild to Moderate Alzheimer's Disease, ClinicalTrials.gov identifier: NCT02386306, Updated February 3, 2016, **https://clinicaltrials.gov/ct2/show/NCT02386306**.
221 Z. Cai, N. Liu, C. Wang, B. Qin, Y. Zhou, M. Xiao, L. Chang, L. J. Yan and B. Zhao, *Cell. Mol. Neurobiol.*, 2016, **36**, 483–495.
222 A. Kumar, L. P. Datta, S. Samanta, H. Arora and T. Govindaraju, *Isr. J. Chem.*, 2021, **61**, 222–230.
223 A. H. Burstein, M. Sabbagh, R. Andrews, C. Valcarce, I. Dunn and L. Altstiel, *Journal of Prevention of Alzheimer's Disease*, 2018, **5**, 149–154.
224 N. D. Prins, J. E. Harrison, H.-M. Chu, K. Blackburn, *et al.*, *Alzheimer's Res. Ther.*, 2021, **13**, 106.
225 M. Ramesh, C. Balachandra, P. Andhare and T. Govindaraju, *ACS Chem. Neurosci.*, 2022, **13**, 2209–2221.
226 J. Han, Z. Du and M. H. Lim, *Acc. Chem. Res.*, 2021, **54**, 3930–3940.
227 S. Park, Y. Yi and M. H. Lim, *Bull. Korean Chem. Soc.*, 2021, **42**, 17–24.
228 M. Kim and M. H. Lim, *Bull. Korean Chem. Soc.*, 2021, **42**, 1272–1280.
229 M. Okuda, Y. Fujita, I. Hijikuro, M. Wada, T. Uemura, Y. Kobayashi, T. Waku, N. Tanaka, T. Nishimoto, Y. Izumi, T. Kume, A. Akaike, T. Takahashi and H. Sugimoto, *J. Alzheimer's Dis.*, 2017, **59**, 313–328.
230 P. Lv, C.-L. Xia, N. Wang, Z.-Q. Liu, Z.-S. Huang and S.-L. Huang, *Bioorg. Med. Chem.*, 2018, **26**, 4693–4705.
231 F. J. Pérez-Areales, O. Di Pietro, A. Espargaró, A. Vallverdú-Queralt, *et al.*, *Bioorg. Med. Chem.*, 2014, **22**, 5298–5307.
232 P. Sharma, A. Tripathi, P. N. Tripathi, S. K. Prajapati, A. Seth, M. K. Tripathi, P. Srivastava, V. Tiwari, S. Krishnamurthy and S. K. Shrivastava, *Eur. J. Med. Chem.*, 2019, **167**, 510–524.
233 Y. Fang, H. Zhou, Q. Gu and J. Xu, *Eur. J. Med. Chem.*, 2019, **167**, 133–145.
234 P. Cai, S.-Q. Fang, X.-L. Yang, J.-J. Wu, Q.-H. Liu, H. Hong, X.-B. Wang and L.-Y. Kong, *ACS Chem. Neurosci.*, 2017, **8**, 2496–2511.
235 P. Cai, S. Q. Fang, H. L. Yang, X. L. Yang, Q. H. Liu, L. Y. Kong and X. B. Wang, *Eur. J. Med. Chem.*, 2018, **157**, 161–176.
236 M. Benchekroun, A. Romero, J. Egea, R. León, P. Michalska, I. Buendía, M. L. Jimeno, D. Jun, J. Janockova, V. Sepsova, O. Soukup, O. M. Bautista-Aguilera, B. Refouvelet, O. Ouari, J. Marco-Contelles and L. Ismaili, *J. Med. Chem.*, 2016, **59**, 9967–9973.
237 F. Prati, A. De Simone, P. Bisignano, A. Armirotti, *et al.*, *Angew. Chem., Int. Ed.*, 2015, **54**, 1578–1582.
238 K. Oukoloff, N. Coquelle, M. Bartolini, M. Naldi, *et al.*, *Eur. J. Med. Chem.*, 2019, **168**, 58–77.
239 L. P. Datta, S. Samanta and T. Govindaraju, *ACS Chem. Neurosci.*, 2020, **11**, 2812–2826.
240 S. Lee, X. Zheng, J. Krishnamoorthy, M. G. Savelieff, H. M. Park, J. R. Brender, J. H. Kim, J. S. Derrick, A. Kochi, H. J. Lee, C. Kim, A. Ramamoorthy, M. T. Bowers and M. H. Lim, *J. Am. Chem. Soc.*, 2014, **136**, 299–310.
241 J. S. Derrick, R. A. Kerr, Y. Nam, S. B. Oh, H. J. Lee, K. G. Earnest, N. Suh, K. L. Peck, M. Ozbil, K. J. Korshavn, A. Ramamoorthy, R. Prabhakar, E. J. Merino, J. Shearer, J.-Y. Lee, B. T. Ruotolo and M. H. Lim, *J. Am. Chem. Soc.*, 2015, **137**, 14785–14797.
242 M. Ramesh, P. Makam, C. Voshavar, H. Khare, K. Rajasekhar, S. Ramakumar and T. Govindaraju, *Org. Biomol. Chem.*, 2018, **16**, 7682–7692.
243 J. Han, H. J. Lee, K. Y. Kim, S. J. C. Lee, J.-M. Suh, J. Cho, J. Chae and M. H. Lim, *ACS Chem. Neurosci.*, 2018, **9**, 800–808.
244 M. Kim, J. Kang, M. Lee, J. Han, G. Nam, E. Tak, M. S. Kim, H. J. Lee, E. Nam, J. Park, S. J. Oh, J.-Y. Lee, J.-Y. Lee, M.-H. Baik and M. H. Lim, *J. Am. Chem. Soc.*, 2020, **142**, 8183–8193.
245 M. H. Park, M. Lee, G. Nam, M. Kim, J. Kang, B. J. Choi, M. S. Jeong, K. H. Park, W. H. Han, E. Tak, M. S. Kim, J. Lee, Y. Lin, Y.-H. Lee, I.-S. Song, M.-K. Choi, J.-Y. Lee, H. K. Jin, J.-s. Bae and M. H. Lim, *Proc. Natl. Acad. Sci. U. S. A.*, 2019, **116**, 23426–23436.
246 M. Kim, M. H. Park, G. Nam, M. Lee, J. Kang, I.-S. Song, M.-K. Choi, H. K. Jin, J.-s. Bae and M. H. Lim, *Mol. Pharm.*, 2021, **18**, 101–112.
247 H.-J. Cho, A. K. Sharma, Y. Zhang, M. L. Gross and L. M. Mirica, *ACS Chem. Neurosci.*, 2020, **11**, 1471–1481.
248 L. Sun, H.-J. Cho, S. Sen, A. S. Arango, T. T. Huynh, Y. Huang, N. Bandara, B. E. Rogers, E. Tajkhorshid and L. M. Mirica, *J. Am. Chem. Soc.*, 2021, **143**, 10462–10476.
249 D. Padhi, C. Balachandra, M. Ramesh and T. Govindaraju, *Chem. Commun.*, 2022, **58**, 6288–6291.
250 A. Mishra, V. Tiwari, S. Singh and S. Shukla, *Experimental models to study Alzheimer's disease in Alzheimer's disease: recent findings in pathophysiology, diagnostic and therapeutic modalities*, Royal Society of Chemistry, 2022, pp. 591–607.
251 P. Rekulapally, L. Garimella, S. Krishnan, N. Ashwin Kumar and S. N. Suresh, *Ethnic and racial differences in the pathophysiology of Alzheimer's disease in Alzheimer's disease: recent findings in pathophysiology, diagnostic and therapeutic modalities*, Royal Society of Chemistry, 2022, pp. 608–659.